Mathias Eriksson

Determining the metamorphic degree around graphite occurrences in the Heinävesi area

Master's thesis

Geology and Mineralogy

Faculty of Science and Engineering

Åbo Akademi University, spring 2019

Mathias Eriksson, 37064

Mathias Eriksson, 2018. *Determening the metamorphic degree around graphite occurences in the Heinävesi area.* This thesis is part of the *Fennoflakes*-project with Åbo Akademi. The studied area is within the exploration section of Beowulf Mining plc.

Keywords: Graphite, metamorphism, eastern Finland, pseudosections, garnet-biotite thermometry

Abstract

The aim of the study is to determine the pressure and temperature conditions around graphite occurences in the Heinävesi area due to the important relationship between metamorphic degree and graphite quality.

Most rocks in the Heinävesi area are quartz-biotite-plagioclase gneisses and biotite paraschists with varying graphite content from disseminated flakes to several percentages. Diatexites and metatexites are common, suggesting partial melting, with occasional garnets, amphiboles and orthopyroxenes.

The rocks are metapelites and greywackes that deposited in a marine-basin created by the break-up of the Neoarchean continent during 2.1-2.05 Ga. The deposition continued until the Svecofennian orogeny when the sediments were thrusted, deformed and metamorphosed by the accretion of the Keitele microcontinent at 1.91 Ga. The metamorphic degree of the rocks has been determined by garnet-biotite thermometry, pseudosections, field observations and thin section analysis. The garnet-biotite thermometry yielded sub-melting temperatures for metapelites (505-640 C°) and is not representative for peak metamorphic temperatures. Due to the observation of diatexites and metatexite a minimum temperature of 650 C° can be concluded. By the occurrence of orthpyroxenes in the thin sections a higher minimum temperature of 750 C° was determined. Pseudosections 015 and 083 yielded a pressure and temperature range of 775-800 C° and 2.8-8 kbar, placing the Heinävesi area in the upper amphibolite facies which is supported by the literature. A high metamorphic degree improves the quality of the graphite making this area suitable for exploration.

Table of contents

Appendices

1 Introduction

Graphite is an increasingly important raw material. It has a wide variety of uses, from common pencils to batteries, heat resistant lubricants and more. From a technological point of view the possibilities of graphene, the one atom thick hexagonal layers within graphite, are of increasing interest. The excellent conductive properties of graphite make it a desired raw material, and the possible extraction of graphene even more so for future applications.

The work in this thesis was performed for a prospecting firm, Fennoscandian Resources Ab, for the Fennoflakes project that focuses on graphite deposits. The goal is to determine the peak pressure and temperature present during the formation of the rocks, since the quality of graphite is highly dependent on the metamorphic degree of the host rock. The area focused on in this thesis is in Eastern Finland in Heinävesi within the Archean domain. The rocks are supracrustal, sedimentary rocks deposited in a marine setting and metamorphosed during the Svecofennian orogeny. Two methods are used to achieve the peak temperature and pressure conditions of the rocks; standard garnet-biotite thermometry and pseudosections. These results are compared with Raman-geothermometry of graphite grains in other theses.

2 Graphite

Graphite is a naturally occurring crystalline form of carbon and is relatively common all around the world. Graphite is characterized by being very soft (<1 Moh scale), leaving marks when rubbed and having a black to metallic grey luster. It has been exploited by mankind for centuries and has many applications of which the most commonly known example might be the pencil. For industrial applications and within the high-tech industry graphite has a very multifaceted use (Olson 2012).

Natural graphite can be classified into three different main types: flake graphite, crystalline (vein) and amorphous graphite. These types differ in physical properties, impurities, chemical composition and appearance, which are determined by the origin material. Flake graphite usually occurs as disseminated flakes in metamorphosed silica-rich quartzites, gneisses and marbles while crystalline graphite occurs in metamorphic and igneous rocks. Amorphous graphite is simply metamorphosed coal (Pierson 1993). Most common host rock is metamorphosed, carbon rich sediments that have gone through reduction and dehydration. The carbon itself usually originates from organic matter but in igneous rocks, where vein graphite occurs, the carbon source is usually C-O-H fluids (Hazen et al. 2013).

For graphite to achieve a fully ordered crystalline structure high temperature and pressure is required, temperature being the more important variable and needs to exceed 400 C°. Graphitization starts in the uppermost greenschist facies to lower amphibolite facies (Landis 1971).

2.1 Properties

Graphite is naturally occurring crystalline carbon where each carbon atom is bonded to three other atoms in a 2D hexagonal pattern. Within this 2D web, each bond is a covalent bond with a strength of 524kJ/mole. The planes are bonded to each other with a much weaker van der Waals bond of 7kJ/mole. This is why graphite is so soft. The individual 2D layers are known as graphene (Pierson 1993).

The metamorphic degree strongly affects the evolution of graphitization. Temperature determines three important properties of the graphitization; Higher temperatures lead to perfection of the individual layer's crystal lattice from an amorphous, poorly ordered structure to a more hexagonal lattice. Increased temperature also decreases the space between the individual graphene layers towards the ultimate spacing of 3.35Å and improves the order of the carbon layers in relation to one another (Landis 1971).

2.2 Graphene

Graphene is the one atom-thick layers within graphite. Graphene flakes display excellent electron and thermal conductivity as well as mechanical strength. Graphene is thought to be the “world’s next wonder material” due to its unique properties, making advanced technological applications possible such as paper-thin tablets, advanced computers, inexpensive solar panels and more (Olson 2012).

2.3 Graphite in Finland

Graphite has been mined in Finland for centuries, but since 1947 production has stopped mainly due to unknown economical deposits, even though the Finnish bedrock is ridden with graphite occurrences (Figure 1). Most of them are in eastern and southern Finland but some occur in northern Finland at the edges of the Lapland granulite belt. Between the years 1760s and 1947, graphite has been mined in about 30 different locations in southern and eastern Finland (Ahtola & Kuusela 2015).

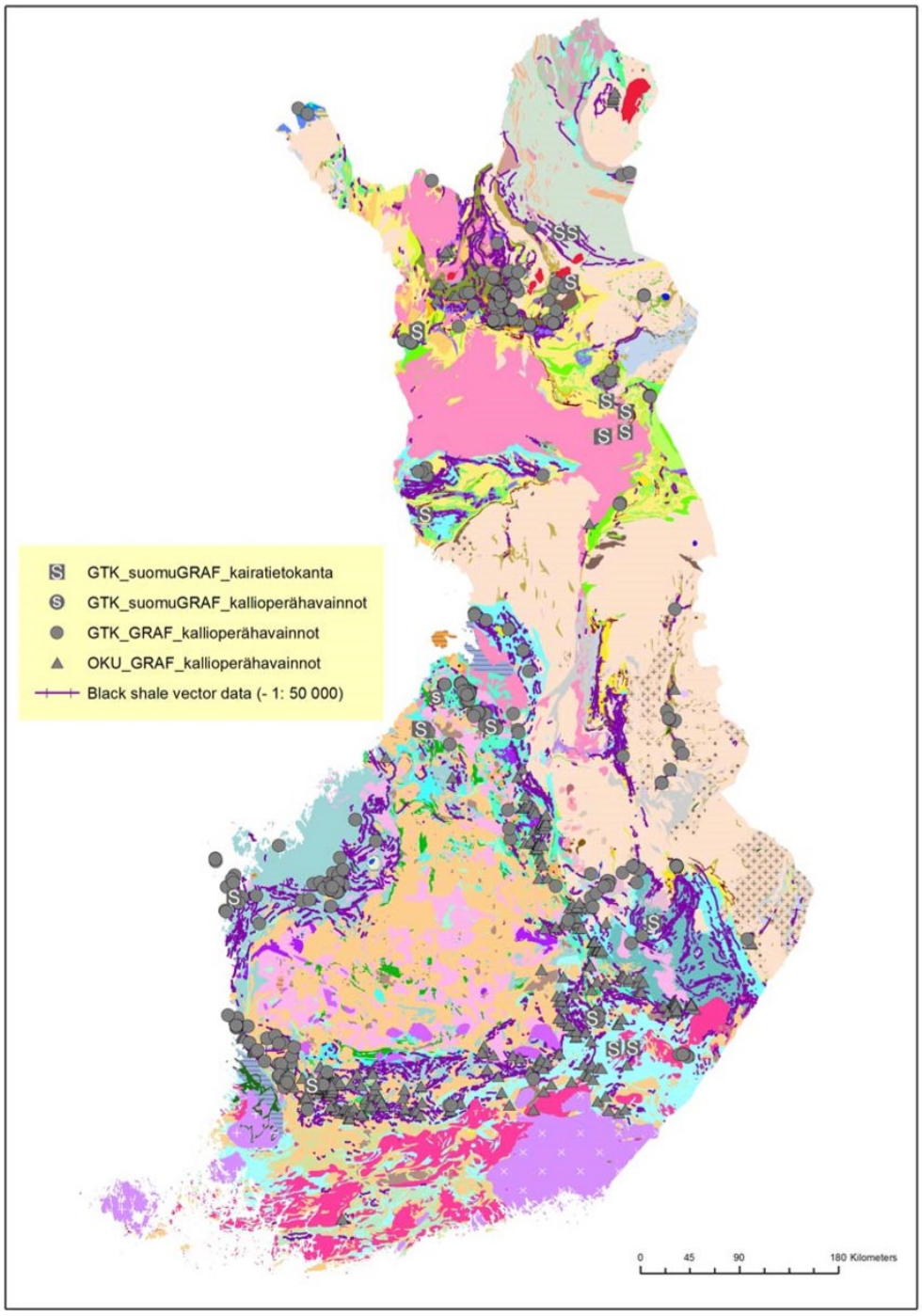

Figure 1. Graphite and black schist occurrences in Finland. Grey dot indicates outcrop observation of graphite, small S indicates vein graphite, grey box indicates graphite found in drill cores and grey triangles symbolize outcrop observations done by Outokumpu (Ahtola, T & Kuusela, J. 2015).

2.4 Uses of graphite and global demand

Graphite is an important material for many industries. Battery producers might be the number one competitor for most available graphite resources. Even though the industry uses synthetic graphite powder too, as the technology develops, the demand for higher grade natural graphite increases as well. Another big graphite consumer are foundries that use large chunks of graphite to make molds for casting whatever is needed, as graphite has a high melting temperature, and molds work well for hot works. Other industries where the high melting temperature of graphite is exploited is when making temperature resistant lubricants and packings. Graphite also increases the pressure tolerance of the lubricant and retains its lubricating effect under high pressure by acting as a solid lubricant film. This is useful for heavy industrial applications such as steel mills or railroads (Kogel et. Al. 2006).

Other uses are pencils, refractories, carbon bushings, bearings, electronics, brake linings, fuel cells and much more (Kogel et Al. 2006).

The demand for graphite is increasing and the material has been placed on the critical raw materials list by the European Commission. The list is a vital part of The Raw Materials Initiative that was launched in 2008 to deal with the upcoming challenges regarding access to critical raw materials. The goal is to ensure a sustainable, secure and affordable supply of materials to meet the needs of the European Union. The list has been updated in 2017 and graphite is constantly on the rise (Figure 2). The parameters used are supply risk and economic importance. Supply risk is determined through the reliability of the supplier and is mostly based on the supplier's governance. Economic importance is determined by the consequences of an eventual inadequate supply of graphite (European Comission 2017).

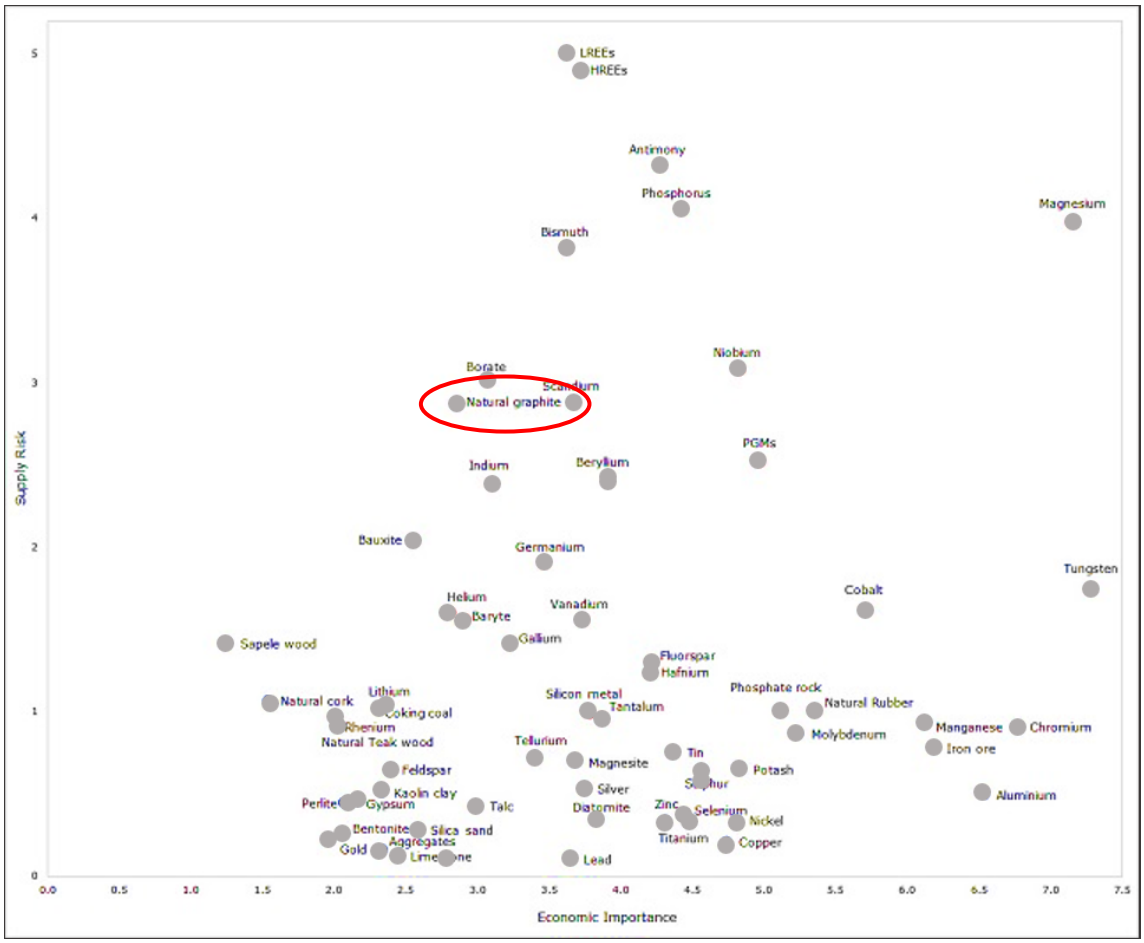

Figure 2. The EU commission's critical raw material list memo from 2017. On the X axis economic importance is plotted and on the Y axis supply risk. Graphite marked with a red circle. (European Commission 2017).

3 Geology

The Fennoscandian shield is an amalgamation of four major lithospheric blocks or tectonic provinces, three microcontinents and some volcanic arcs. The two fundamental events in the evolution of Fennoscandia are the break-up of the Archean continent and amalgamation of the four lithospheric blocks (Karelia, Lapland-Kola, Norrbotten and Svecofennia provinces). The break-up occurred at 2.1-2.05 Ga and amalgamation of the blocks at 1.92-1.86 Ga through collisions of the Karelian craton, Norrbotten continent,

Knaften arc, Keitele microcontinent, Bergslagen microcontinent, Bothnian microcontinent and Volgo-Sarmantia (Niironen 2017).

The Neoarchean continent assembly occurred at 3.1-2.68 Ga, consisting of two colliding Archean cratons. The continental core nucleuses are known as the Karelia and Murmansk nucleus. The amalgamation created the Karelian and Lapland-Kola provinces, as well as the Belamorian mountain range (Niironen 2017).

These are greenstone belts are found within the Karelian province and are believed to have originated from arc magmatism. Accretion of the cratons occurred at 2.83-2.75 Ga, crustal stacking and the genesis of the Neoarchean continent at 2.73-2.68 Ga (Niironen 2017).

From 2.68-2.1 Ga extensional events took place within the Neoarchean continent/Karelian craton, which finally led to complete break-up at 2.1-2.05 Ga. The basins created during this break-up are the deposition location of the Kaleva system rocks (Niironen 2017).

During 1.92-1.87 Ga the main collisional stage took place. At 1.93-1.92 Ga blocks of Archean crust collided with the Karelian craton. The mountain belt created by this collision could be the source material for the Kaleva system rocks. The subduction caused metamorphism of the Lapland granulite belt at high pressures and Paleoproterozoic overprinting on Archean structures (Niironen 2017)

The initiation of the Svecofennian orogeny began at 1.92 Ga when the continental blocks Karelia and Norrbotten collided along with the Knaften volcanic arc and Keitele microcontinent. The accretion of the Ketiele microcontinent resulted in slab break-off and polarity reversal of the subduction along the Norrbotten margin. The Keitele microcontinent accretion also resulted in metamorphism of the Kaleva sediments at 1.91 Ga (Niironen 2017).

At 1.88-1.87 Ga the amalgamation of the microcontinents Bothnia and Bergslagen, finalizing the assembly of the protocontinent Fennoscandia (Niironen 2017).

From 1.86-1.83 Ga the protocontinent entered a stabilization phase and crustal extension period. High heat flow derived from the mantle caused high temperature metamorphic conditions and concurrent granite magmatism (Niironen 2017).

The final collision occurred at 1.84-1.80 Ga. The Volgo-Sarmatia and proto Fennoscandia continents collided in an oblique manner, causing the Svecobaltic orogeny and genesis of the Baltica continent (East European craton). The magmatism following the collision produced the Transscandinavian Igenous Belt (TIB), although it is discussed if the TIB is caused by a collision with the Amazonia continent as well. During 1.81-1.77 Ga post-collisional magmatism took place, producing shoshonitic rocks and pegmatites (Niironen 2017).

Fennoscandia entered a crustal stabilization period from 1.76 to 1.65 Ga. On the southwestern margin TIB magmatism was produced due to continuous accretionary orogenic activity and at 1.65 Ga initation of intracontinental rifting began. Rapakivis, dyke swarms and sedimentation occurred during this phase (Niironen 2017).

3.1 Metamorphic events within Fennoscandia

The Finnish bedrock has a metamorphic history of different ages and metamorphic grades ranging from low to high. The Archean bedrock was metamorphosed during 2.70-2.60 Ga in upper-amphibolite facies with pressures ranging from 6-7 kbar, excluding the greenstone belts which were metamorphosed at mid-amphibolite facies with a common pressure range of of 5-6 kbar. The majority of the Archean bedrock has been overprinted by Paleoproterozoic metamorphism, especially near Paleoproterozoic shear zones within the Archean bedrock. The reheating is associated with the burial of the Archean bedrock by the nappe complexes at 1.9 Ga. A small amount of Mesoproterozoic sedimentary rocks occur and are of sub-greenschist facies (Hölttä & Heilimo, 2017).

The Keitele microcontinent accretion resulted in metamorphism of the Kaleva sediments at 1.91 Ga (Niironen 2017) which is relevant for this thesis. The Kaleva sediments, which belong to the North Karelian schist belt, show a westward increasing metamorphic degree. Signs of rapid exhumation has been observed by staurolite co-existing with cordierite and andalusite, minerals that do not share the same pressure and temperature equilibrium conditions (Hölttä & Heilimo, 2017).

The Svecofennia province experienced metamorphic degrees of upper-amphibolite facies to granulite facies at pressures from 4-6 kbar, with temperatures ranging from

700-880 C°, (Hölttä & Heilimo, 2017) during the peak metamorphism when microcontinents Bergslagen and Bothnia collided with proto Fennoscandia (Niironen 2017). The Svecofennia province shows an abundance of metatexitic and diatexitic migmatites (Hölttä & Heilimo, 2017).

3.2 Area description

The studied area is located in Leppävirta municipality which lies 50 kilometers south east of eastern Finland's biggest town, Kuopio (Figure 3). The area is a typical eastern Finland farmland with relatively sparse inhabitants. The road network is well developed even within the forested areas.

The area belongs to the upper Kaleva tectofacies, an allochtonous marine basin, within the Karelian province. These rocks have been metamorphosed during the Svecofennian orogeny around 1.91 Ga due to the collision with the Keitele microcontinent (Niironen 2017). The lower to upper Kaleva units represent the initial stages of the Svecofennian orogeny, when the foredeep to foreland Kaleva deposits were thrusted into complex allochtons during 1.95-1.92 Ga (Niironen 2017).

The rocks in the upper Kaleva unit consists of metamorphosed sedimentary rocks such as psammites, pelites and greywackes deposited in deep water as turbiditic currents and mass flows. The sedimentary material is mainly Archean but has also characteristics of primitive Proterozoic substrates. The maximal depositional age varies for the upper Kaleva unit but has been approximated to be 1.939 and 1.924 Ga, depending on locality. Despite the age discrepancy the rocks are considered to be part of the same large-scale depositional system. The marine basin in which the material deposited opened during 2.1-2.05 Ga by the break-up of the Neoarchean continent (Niironen 2017). The deposition of material has been continuous during the Svecofennian orogeny (Laajoki et al. 2005).

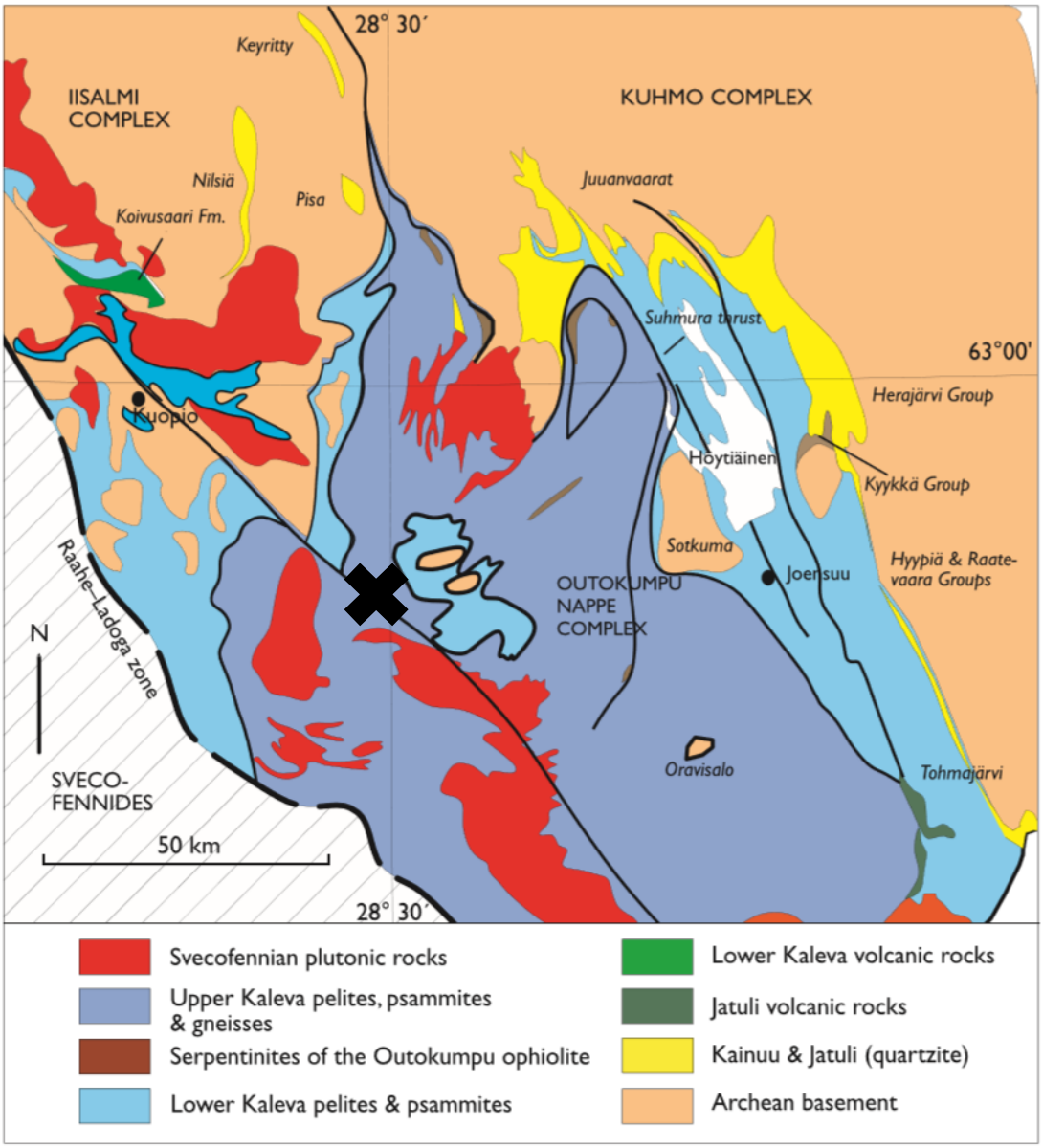

Figure 3. Simplified geological map of North Karelia and Eastern Savo. (Laajoki, K. et. al. 2005). The studied area is marked with a black cross within the upper Kaleva facies.

4 Field work and site description

The field work was executed in eastern Finland near Heinävesi during spring and summer of 2017. Three different areas were mapped on three separate occasions. The first area, Haapamäki, lies near the Haapamäki fold hinge. The second area is known as Rääpysjärvi and the third area Kohmansalo.

Graphite was of particular interest and can be identified by its grey luster and staining when rubbed. Disseminated graphite was common at several sites and individual grains could be identified in varying grain size. Sampling was done primarily with regard to graphite content but also to achieve an even spread of samples across the study areas.

Concurrently with the detailed bedrock mapping, conductivity measurements were done with a *mini-slingram Double Dipole APEX Mark II* conductivity gauge to locate conductive anomalies. Black schists appear as highly conductive anomalies since graphite is a very conductive mineral.

The Slingram is an electromagnetic instrument initially developed for mining explorations to locate conductive materials but is widely used for ground water and archeological research as well as engineering problems. A typical Slingram instrument consists of a transmitter in the front and a receiver in the back. The transmitter emits an electromagnetic field that is picked up by the receiver in the rear. As the signal passes through a conductive material it is altered into a secondary field. The intensity and properties of the secondary field is depending on the conductive material, depth of overburden, signal strength and orientation of the material (Nabighian 1991).

Detailed bedrock mapping was done, with standard equipment and sampling was done with a hammer. In total 180 observations were done of which 65 contained graphite (appendix).

The area shows a large fold structure with an axial plane pointing roughly NW as seen in the lithological map in Figure 4 and electromagnetic map in Figure 5.

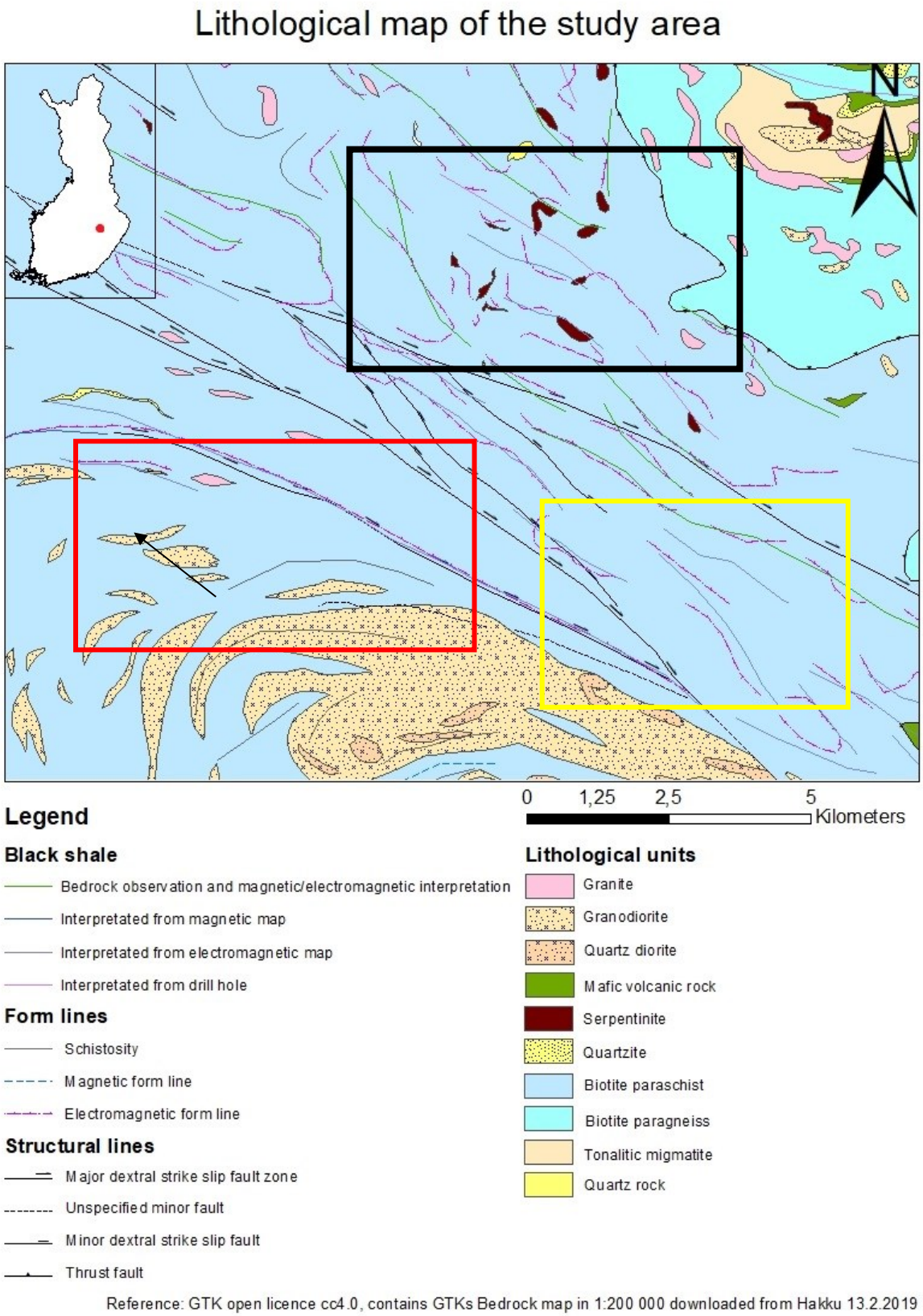

Figure 4. Lithological map of the study area. The red square indicates Haapamäki, the black Rääpysjärvi and the yellow Kohmansalo. The black arrow shows the orientation of the axial plane.

4.1 Haapamäki

Haapamäki area lies close to the Haapamäki fold hinge and shows a strong electromagnetic anomaly (Figure 5) The detailed bedrock mapping was focused within this anomaly and in total 67 sites were mapped. Since the area is relatively well exposed most observations could be done on outcrop and subcrop. The foliation lies in a NW-SE fashion with a dip between 70 to 88.

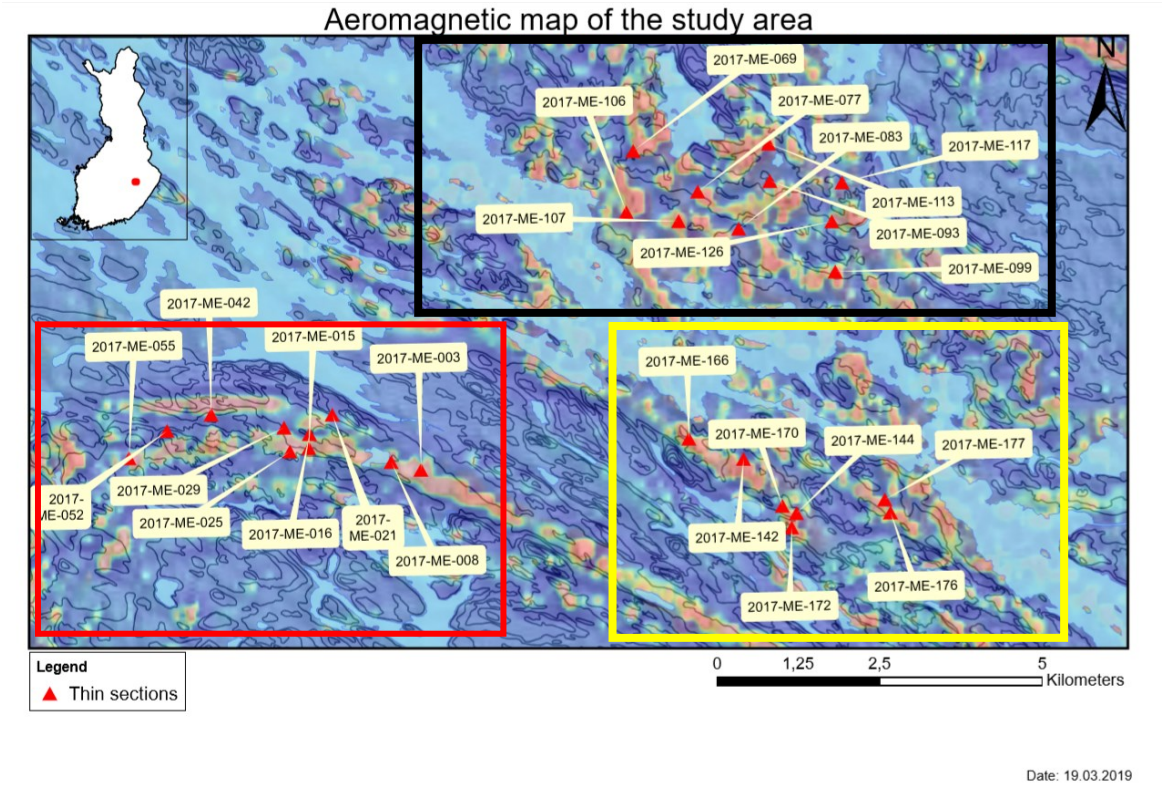

Figure 5. Electromagnetic map of the exploration area with sample sites of samples made into thin sections. Colored squares indicate the study areas. Red is Haapamäki, black Rääpysjärvi and yellow Kohmansalo.

The area consists mostly of biotite paraschist with a varying degree of migmatization and deformation. Most outcrops are weathered and rusty due to sulfide oxidation. Diatexitic (Figure 6A) and metatexitic textures are common (Figure 6B).

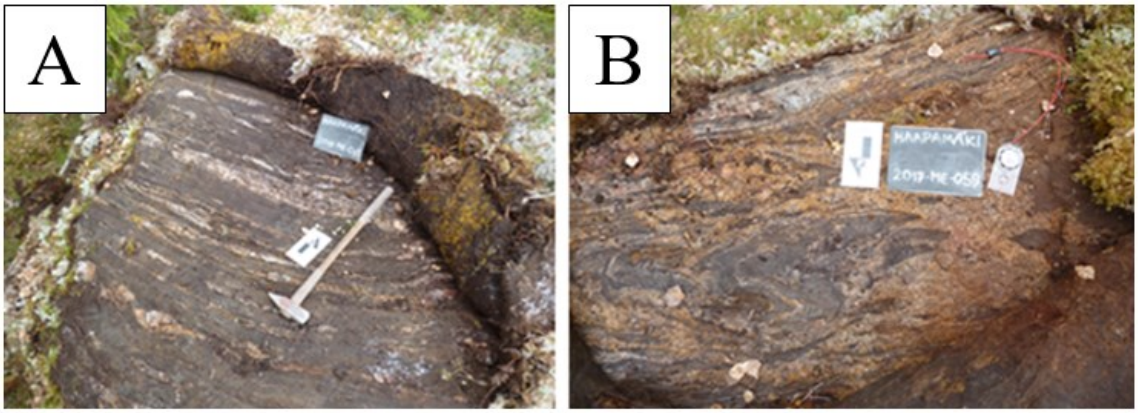

Figure 6. Varieties of migmatites in Haapamäki. Metatexite 6A, diatexite 6B.

4.2 Rääpysjärvi

The Rääpysjärvi area lies about 10 km NE of the Haapamäki fold hinge and shows no uniform electromagnetic anomaly but rather scattered individual smaller anomalies (Figure 5). The bedrock mapping was focused around and within these smaller anomalies. In this area 59 sites were mapped, a third of them on boulders, since the exposure level was poor. The main rock type was quartz-feldspar-biotite gneiss (QFB gneiss) with relative abundance of garnet. 59 sites were mapped and 20 contained graphite.

4.3 Kohmansalo

The Kohmansalo area shows scattered electromagnetic anomalies lying in roughly NW-SE fashion. The area is more migmatitic compared to the two other areas. The exposure level was decent despite having several farming fields in the topographic lows, usually concentrated in the high electromagnetic anomalies. Main rock type was QFB gneiss with observed apatite at some sites.

5 Materials and methods

The gathered material consists of 180 field observations and 80 hand samples, primarily selected by graphite content and deviating mineralogical properties.

Two different methods were used to determine the temperature and pressure ranges of the rocks. Garnet-biotite thermometry and pseudosections. In order to do these analyses thin section examination, bulk-chemical analysis through X-ray fluorescence (XRF) and micro probing were done. Scanning electron microscopy (SEM) was used to complement the thin section analysis.

5.1 Thin sections and petrographic studies

Out of 80 field samples 27 were made into polished thin sections (table 1). 10 from Haapamäki and Kohmansalo and 7 from Rääpysjärvi. The thin sections are 30µm thick, cut perpendicularly against the foliation and polished which allows further analyses to be made in determining the pressure and temperature conditions of the rocks. The EDS was used to identify minerals that could not be identified through polarizing microscopy.

Table 1. List of thin sections. Further analyses have been done on the samples with an asterisk (*).

OBS_ID	PROSPECT	LOCATION	EASTING	NORTHING
2017-ME-003	Haapamäki	Kuolemanmäki	3572100	6941246
2017-ME-008	Haapamäki	Kuolemanmäki	3571644	6941360
2017-ME-015*	Haapamäki	Kalliokumpu	3570373	6941575
2017-ME-016	Haapamäki	Kalliokumpu	3570382	6941792
2017-ME-021	Haapamäki	Kalliokumpu	3570735	6942091
2017-ME-025*	Haapamäki	Kaituransalo	3570086	6941523
2017-ME-029*	Haapamäki	Kaituransalo	3569994	6941893
2017-ME-042	Haapamäki	Kaituransalo	3568872	6942088

2017-ME-052	Haapamäki	Haukisalo	3568195	6941840
2017-ME-055	Haapamäki	Haukisalo	3567608	6941423
2017-ME-069	Rääpysjärvi	Torpanpelto	3575362	6946140
2017-ME-077	Rääpysjärvi	Hiekkalahdenmäki	3576357	6945513
2017-ME-083*	Rääpysjärvi	Torpanpelto	3576988	6944947
2017-ME-093	Rääpysjärvi	Laukansalo	3577468	6945679
2017-ME-099*	Rääpysjärvi	Laukansalo	3578471	6944290
2017-ME-106	Rääpysjärvi	Suurisuo	3575259	6945200
2017-ME-107	Rääpysjärvi	Suurisuo	3576063	6945061
2017-ME-113*	Rääpysjärvi	Hiekkalahdenkangas	3577447	6946256
2017-ME-117	Rääpysjärvi	Hiekkalahdenkangas	3578577	6945656
2017-ME-126	Rääpysjärvi	Laukansalo	3578420	6945057
2017-ME-142	Kohmansalo	Kohma	3577057	6941412
2017-ME-144	Kohmansalo	Kohma	3577875	6940575
2017-ME-166*	Kohmansalo	Kohma	3576221	6941721
2017-ME-170	Kohmansalo	Kohma	3577660	6940690
2017-ME-172	Kohmansalo	Kohma	3577802	6940356
2017-ME-176	Kohmansalo	Rusinvirta	3579317	6940586
2017-ME-177*	Kohmansalo	Rusinvirta	3579233	6940784

5.2 Scanning electron microscope (SEM)

The instrument used was a SEM JEOL JSM-IT 100 with two detectors; Back scattered electron (BSE) and energy-dispersive X-ray spectroscopy (EDS). The thin sections were carbon coated to enhance the conductivity of the material prior to SEM and Electron Micro-Probe analyses. Samples analyzed with the SEM are listed in table 2.

Table 2. List of samples analyzed with the SEM.

OBS_ID	SEM
2017-ME-015	x
2017-ME-025	x
2017-ME-029	x
2017-ME-099	x
2017-ME-166	x

A SEM works by focusing a beam of high energy electrons on the material of interest. The electron interactions between the beam and the material give rise to specific signals that are picked up by the detectors (Swapp 2017). The common signals used to create an image of the material are back-scattered electrons, secondary electrons and Auger electrons. Some electrons of the beam pass right through the material and do not create a signal. X-rays and cathodoluminisence signals are also generated and picked up. However, the Auger and secondary electrons give rise to the highest resolution of imaging compared to other signals (Henry 2016). SEM is also capable to semi-quantitatively determine elemental compositions of the material of interest using the EDS (Swapp 2017).

5.3 Electron Microprobe

The instrument used was an electron micro probe JEOL JXA-8600 with three spectrometers whereas three were used; the TAP, PET and LiF for quantitative elemental analysis. Biotite, garnet, kaerstutite and albite were used as reference minerals. The analysis was conducted by MSc. Casimir Näsi at Top Analytica Oy Ab in Turku, Finland. Samples containing garnet biotite or amphibole plagioclase pairs were analyzed with the Electron Micro-Probe and are listed in table 3.

Table 3. List of samples analyzed with the Electron Micro-Probe.

OBS_ID	Amph+plag	Grt+bt
2017-ME-015	x	
2017-ME-025		
2017-ME-029		x
2017-ME-083		x
2017-ME-099		
2017-ME-113		x
2017-ME-166	x	
2017-ME-177		x

An electron micro probe works by the fundamentals of emitted x-rays and derivative electrons from the material bombarded with a concentrated beam of accelerated electrons. The beam is fired from an electron source, usually a wolfram-filament cathode. The beam is concentrated by electromagnetic lenses to acquire a precise and narrow beam, usually one to two microns wide. The emitted rays and electrons from the analyzed material are characteristic depending on the elemental composition. The emitted energy and wavelength- dispersive beams are picked up by the spectrometers giving a unique signal to each element present. A micro probe is excellent for most chemical analyses but lighter elements such as H, He, Li or O are not detected (Goodge 2017).

5.4 X-ray fluorescence & Micro-X-ray fluorescence

The instrument used was a Micro-XRF, M4 TORNADO. The analysis was conducted by lab engineer Sören Fröjdö at Geology and Mineralogy, Åbo Akademi University. Samples analyzed are listed in Table 3.

Table 3. List of samples analyzed with the XRF.

OBS_ID	Micro-XRF
2017-ME-015	x
2017-ME-083	x
2017-ME-166	x
2017-ME-177	x

Prior to the XRF analysis the grab samples were crushed using a Fritsch Pulverisette jaw-crusher and pulverized using a Siebtechnik vibratory disc mill. The powder was left to dry in ~100 °C overnight. The powder was made into compressed powder pucks and glass pucks. For the compressed pucks 2 g of wax was mixed with 8 g of sample powder. The mix was compressed with a hydraulic press with a pressure of 20 t. The powders for the glass pucks were oxidized in >1000 °C. After cooling, 1.5 g of sample was mixed with 10.5 g of $LiBO_2$. The mixture was heated to ~1500 °C to produce melt which was casted into glass pucks.

The XRF method is based on fluorescent waves emitted from the analyzed material when bombarded with high-energy X-rays. When the electrons of the atoms interact with the emitted high energy X-rays, the electron or electrons of the outer orbital ejects, ionizing the atom. If the energy delivered through X-rays is greater than the ionizing energy of the atom, electrons within the inner orbitals can be ejected. To establish equilibrium, electrons of the outer orbitals replace the missing electrons in the inner orbitals. During this jump from outer to inner orbitals the electrons emit a lower energy radiation, i.e the fluorescent radiation. The photons emitted during this transition are characteristic to each element and can therefore be identified (Wirth & Barth, 2019).

The difference between conventional XRF and micro-XRF is that a micro-XRF makes use of optics to focus the X-ray beam to a small spot in order to selectively analyze specific features of the sample, while a conventional XRF has no optics and uses a non-focused, wider beam. (Behrends & Kleingeld, 2009)

The XRF is well suited for bulk chemical analyses for both major elements and trace elements (Wirth & Barth, 2019). In this study XRF was used to determine the bulk chemical composition of the rock in order to build pseudosections for determining the pressure and temperature conditions of the rock.

5.5 Garnet-Biotite thermometry

Garnet-biotite thermometry is based on Fe and Mg partitioning between the mineral pairs. The amount of iron and magnesium varies depending on the temperature during mineral growth. (Ferry & Spear 1978). To determine the temperature of the rock, the rock analysis is compared to a set of artificial mineral assemblages where the temperature is known. To accurately gain a realistic temperature, different calibrations are used to accommodate for defects in the mineral pairs and variations in chemical partitioning (Holdaway et al., 1997).

For this garnet-biotite study, four calibrations were used. Bhatt et al 92, Hodges and Spear as well as Thompson 76 using a Garnet-Biotite Microsoft Excel calculation spreadsheet

provided by University of Oxford's Earth Sciences web page, Practical Aspects of Mineral Thermobarometry 2004.

Beam current used was 20nA with an acceleration voltage of 15kV. Peak analysis time was 25 seconds with a background analysis of 5 seconds.

5.6 Pseudosections and Perple_X

Pseudosections are equilibrium phase diagrams from which the temperature and pressure conditions of the rock can be determined. Pseudosections are built using whole rock chemical data as well as mineralogical data to show fields of stable phase assemblages as opposed to chemical reactions in standard phase diagrams (Hirsch et al., 2016).

Perple_X is a software used for building pseudosections or calculating rock modal properties. It is a thermodynamic calculation package that uses thermodynamic databases and activity models for minerals, liquids and melts. The calculations rely on Gibbs minimum energy, the lowest possible energy level for the compounds to exist in. For solid-solution minerals the program divides the minerals into pseudocompounds to address the behavior of energy equilibrium in a solid state (Hirsch & Baldwin, 2016).

For constructing pseudosections, whole rock chemical data from the XRF analysis was used. Once the chemical data were entered into the program along with the known minerals seen in thin sections, the software calculates all possible mineral assemblages the rock could theoretically contain within the chosen pressure and temperature range.

6 Results

6.1 Field work

Within the exploration area the main rock is biotite paraschist with a mineral composition of quartz, feldspar (mainly plagioclase) and biotite. The field name used is QFB-gneiss. Most sites have traces of graphite with field estimated content of 1-8%.

Migmatites are relatively common in the area and are observed at several sites. Rocks with metapelitic or greywacke compositions begin migmatization at 650 °C (Hölttä & Heilimo 2017) which gives a minimum temperature of the area.

6.2 Petrography

All thin sections show similar mineralogical composition of quartz, plagioclase and biotite with the exceptions of samples 015, 016 and 166. Thin sections 015 and 166 contain hornblende as a main mineral and orthopyroxene as accessory. The occurrence of orthopyroxene gives a minimum temperature of 750 °C, since orthopyroxene in greywacke compositions has a stability field of above 750 °C with a pressure range of 0-9 kbar (Hölttä & Heilimo 2017).

Accessory minerals encompass graphite, garnet, orthopyroxene, epidote, rutile, ilmenite, apatite and zircons. Common alterations are sericitation of feldspar and dehydration rims on biotite. Mineralogical composition of all thin sections can be seen in Table 4. The thin sections which have been used for thermometry and pseudosections are described in detail below.

Table 4. List of minreals observed in all thin sections.

Sample	Main mineral	Accessory minerals
2017-ME-003	Plag,bt, qz	graph
2017-ME-008	Qz, plag, graph	bt
2017-ME-015	Qz, hbl, plag	Opx, graph, bt, grt, ilm
2017-ME-016	Qz, fsp (ortho+micro)	bt
2017-ME-021	Plag, bt, qz	graph, grt
2017-ME-025	Qz, plag, bt	grt, zr
2017-ME-029	Qz, plag, bt	grt
2017-ME-042	Qz, plag, bt	grt
2017-ME-052	Qz, plag, bt	graph

2017-ME-055	Qz, bt, plag	grt, zr
2017-ME-069	Qz, bt, plag	graph, grt
2017-ME-077	Bt, plag, qz	zr
2017-ME-083	Qz, plag, bt	graph, grt, zr, ap
2017-ME-093	Plag, gz, bt	
2017-ME-099	Plag, qz, bt	grt, ap
2017-ME-106	Qz, plag, bt	graph
2017-ME-107	Plag, qz, bt	graph, zr
2017-ME-113	Plag, qz, bt	Graph, grt
2017-ME-117	Qz, plag, bt	
2017-ME-126	Qz, plag, graph	bt
2017-ME-142	Qz, plag, bt	
2017-ME-144	missing	
2017-ME-166	Hbl, plag, bt	qz, opx
2017-ME-170	Qz, plag, bt	graph, epi
2017-ME-172	Qz, plag, bt	
2017-ME-176	Qz, plag, bt	graph, rt
2017-ME-177	Qz, plag, bt	grt

6.2.1 Thin section Haapamäki 2017-ME-015

In thin section 015 the main minerals are quartz, hornblende and plagioclase with accessory minerals orthopyroxene, biotite and garnet (Figure 7). Opaque minerals include graphite and ilmenite. Weak sericitation on plagioclases and undulating quartz grains are common.

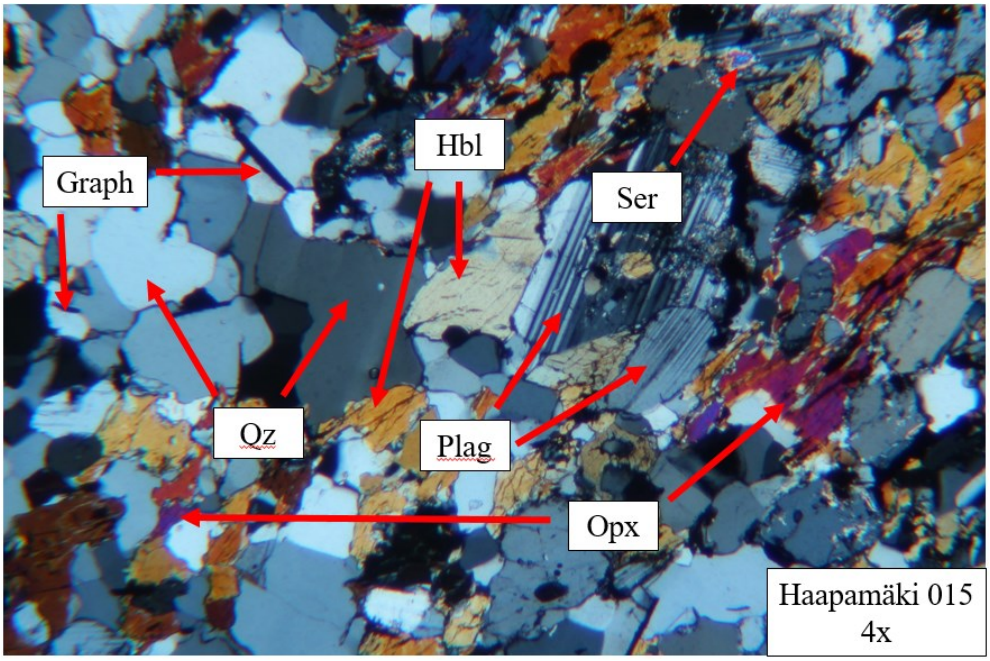

Figure 7. Thin section 015 in cross polarized view. Hornblende, plagioclase, quartz, orthopyroxene, graphite and sericitation visible.

6.2.2 Thin section Haapamäki 2017-ME-025

The main minerals are quartz, biotite and plagioclase with accessory minerals as garnet, zircons and pumpellyite. The pumpellyite occurs as a fibrious blue mineral within biotite grains. Formed during retrograde metamorphism at 3-4 kbar and 300-400 °C. Sericitation of plagioclase is common.

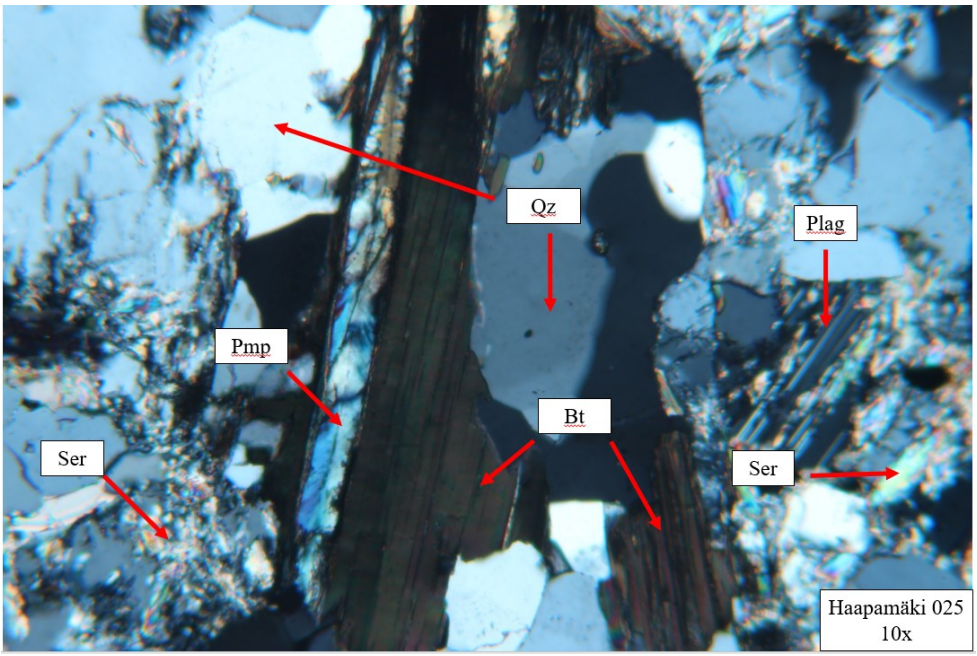

Figure 8. Thin section 025 in cross polarized view. Quartz, biotite, plagioclase, sericitation and pumpellyite marked with red arrows.

6.2.3 Thin section Haapamäki 2017-ME-029

The main minerals are quartz, biotite and plagioclase with garnet as accessory. Biotite shows a range of interference colors and dehydration rims. One mineral could not be identified (Figure 9).

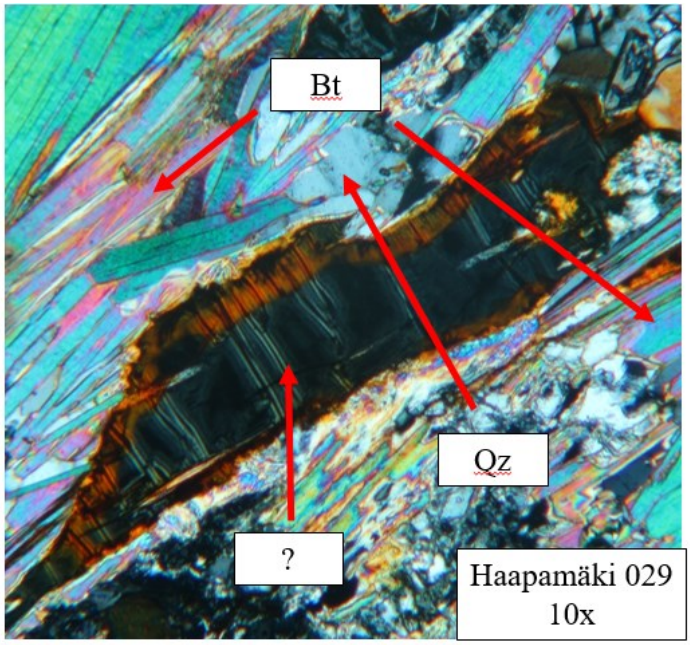

Figur 9. Thin section 029. Unknown minreal in cross polarized view with discolored biotite and quartz grains.

6.2.4 Thin section Rääpysjärvi 2017-ME-083

Main minerals include quartz, biotite and plagioclase with graphite, garnet, apatite and zircon as accessory minerals (Figure 10). Precipitated graphite is seen as graphite flakes with a smooth and a rugged side, usually bordering quartz grains. Volatile inclusions are seen in the quartz grains bordering the precipitated graphite flakes (Figure 11).

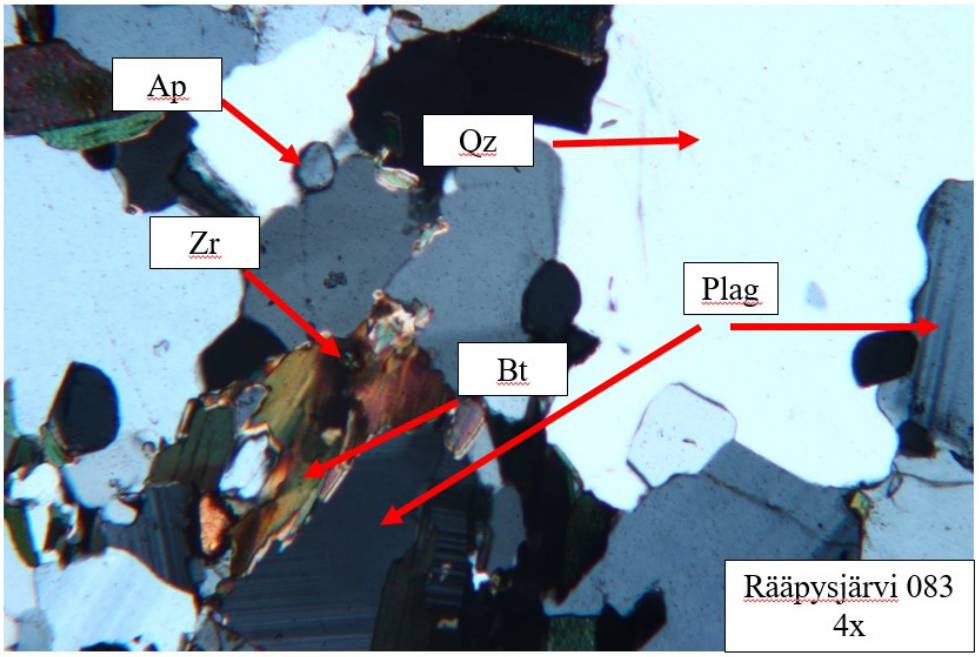

Figure 10. Thin section 083 in cross polarized view. Plagioclase, quartz and biotite, with zircons within the biotite, and small apatite grains.

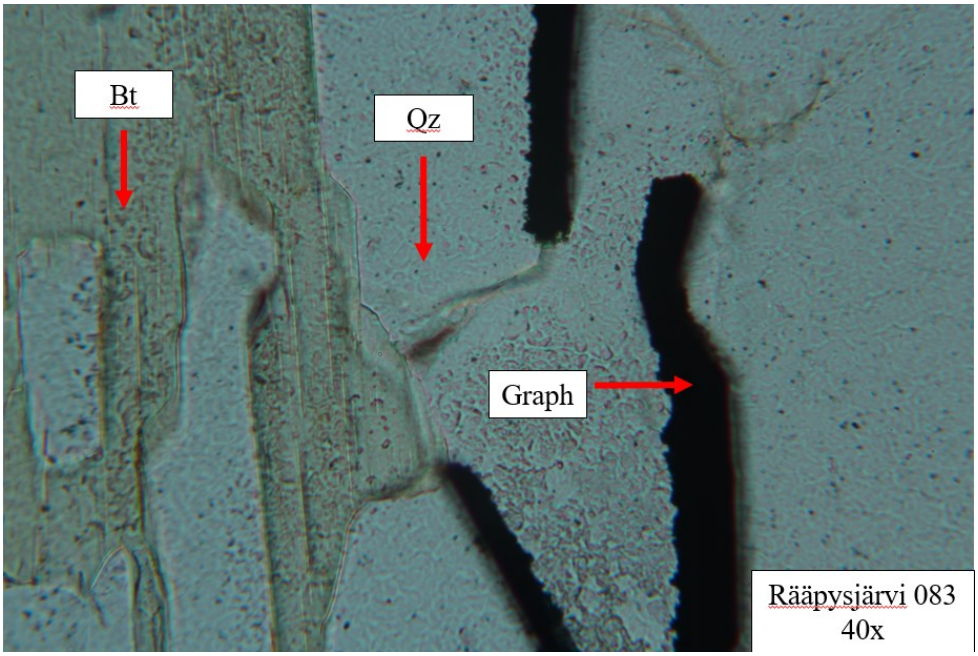

Figure 11. Thin section 083 in plane polarized view. Volatile precipitated graphite along quartz grain boundaries.

6.2.5 Thin section Rääpysjärvi 2017-ME-113

Main minerals include quartz, biotite and sericitated plagioclase with graphite, garnet, and zircon as accessory minerals (Figure 12). The sample is similar to 083.

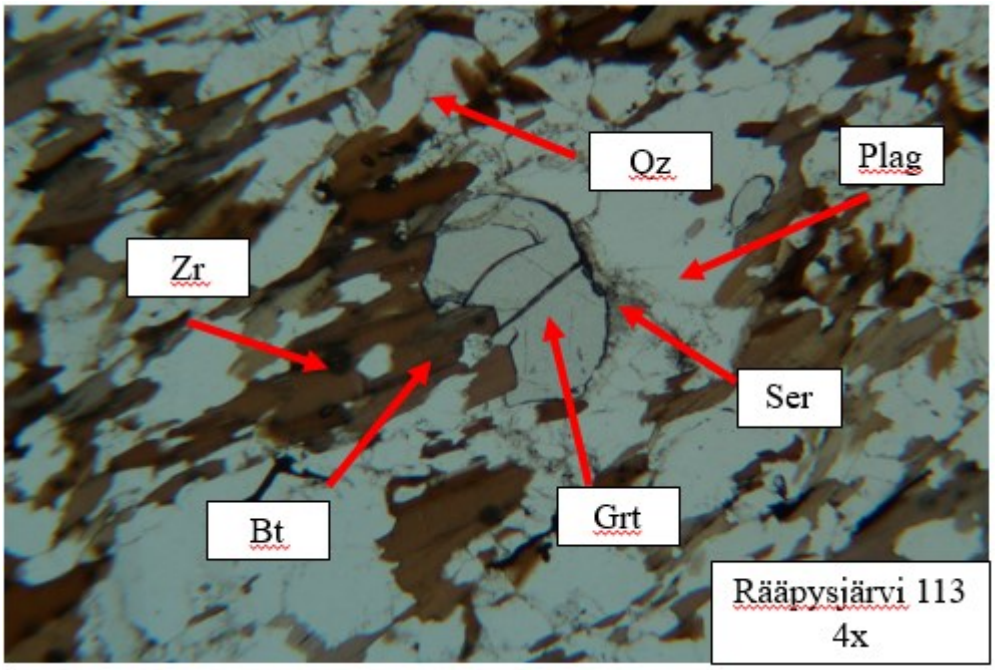

Figure 12. Thin section 113 in plane polarized view. Biotite, quartz, plagioclase, garnet, zircons and sericitation visible.

6.2.6 Thin section Kohmansalo 2017-ME-166

Main minerals include hornblende, biotite and plagioclase with quartz and orthopyroxene as accessory minerals. The biotite is disturbed and shows a range of pink, blue and yellow interference colors (Figure 13). Orthopyroxene occurs as large broken grains (Figure 14).

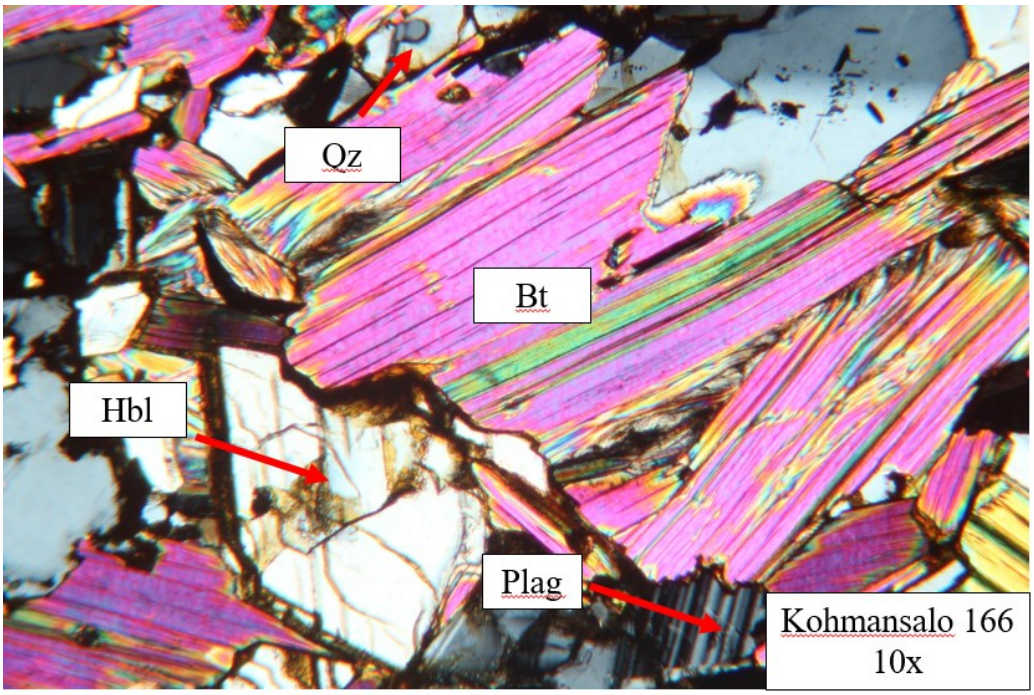

Figure 13. Cross polarized view of thin section 166. Biotite, hornblende, plagioclase and quartz visible. Biotite heavily disturbed.

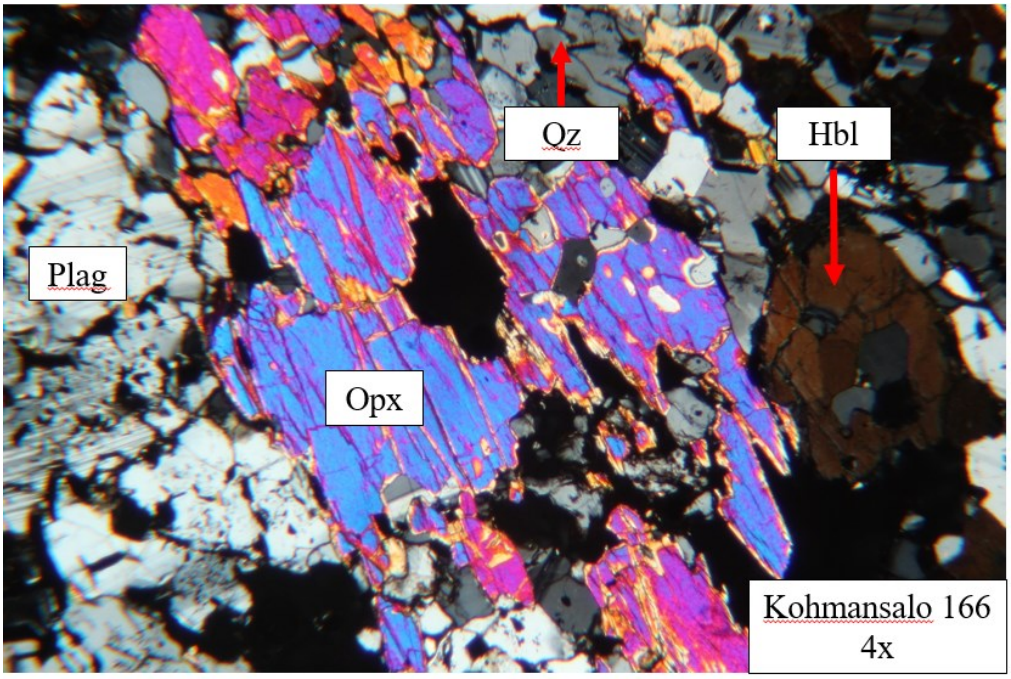

Figure 14. Cross polarized view of thin section 166. Large orthopyroxene grain seen in the middle with plagioclase, quartz and hornblende in the surroundings.

6.2.7 Thin section Kohmansalo 2017-ME-172

The main minerals include again plagioclase, quartz and biotite. Melt escape channels can be observed (Figure 15).

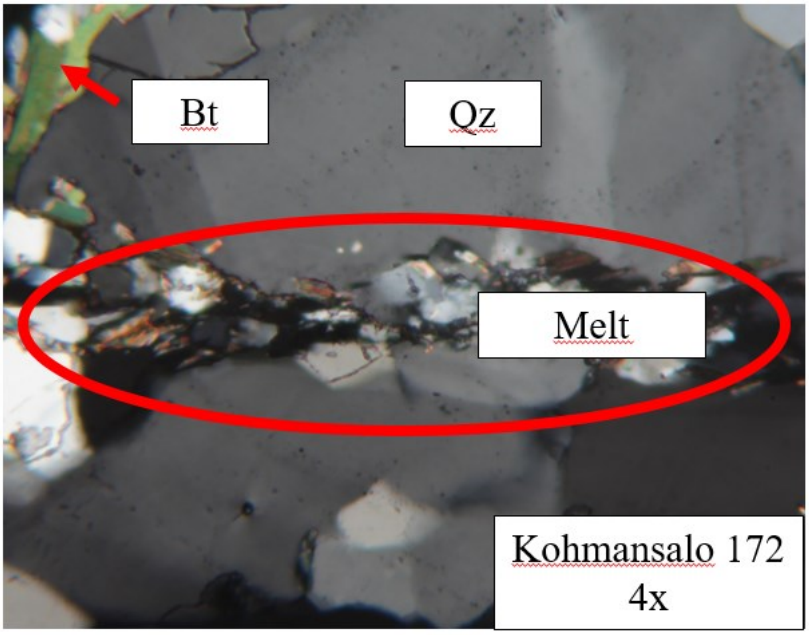

Figur 15. Cross polarized view of thin section 172. The red circle marks a melt escape channel.

6.2.8 Thin section Kohmansalo 2017-ME-177

Main minerals include quartz, plagioclase and biotite with garnet as acessory. Biotite shifts in color towards green (Figure 16).

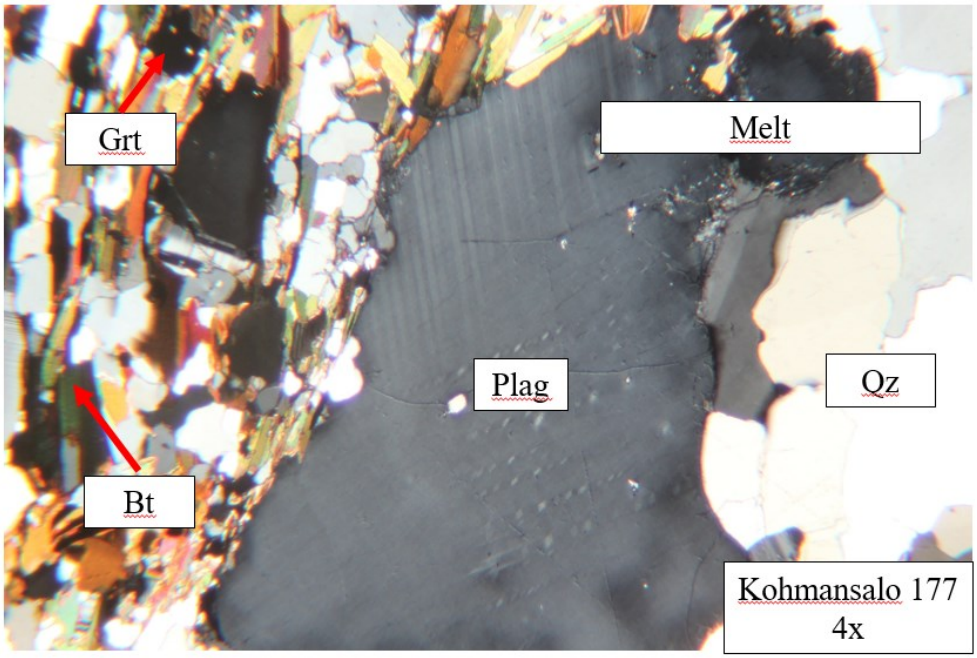

Figure 16. Cross polarized view of thin section 177. Crystallized melt to the right.

6.3 SEM

For thin section 015, orthopyroxene was identified through microscopy and confirmed by EDS. Ilmenite was identified as well. In thin section 025 pumpellyite was identified but the unidentified mineral in thin section 029 remains unidentified. Spectras for respective minerals seen (Figures 17-19). For thin section 099 apatite was identified and in 166 hornblende and orthopyroxene confirmed, EDS spectras for the amphiboles and orthopyroxenes seen in the appendix.

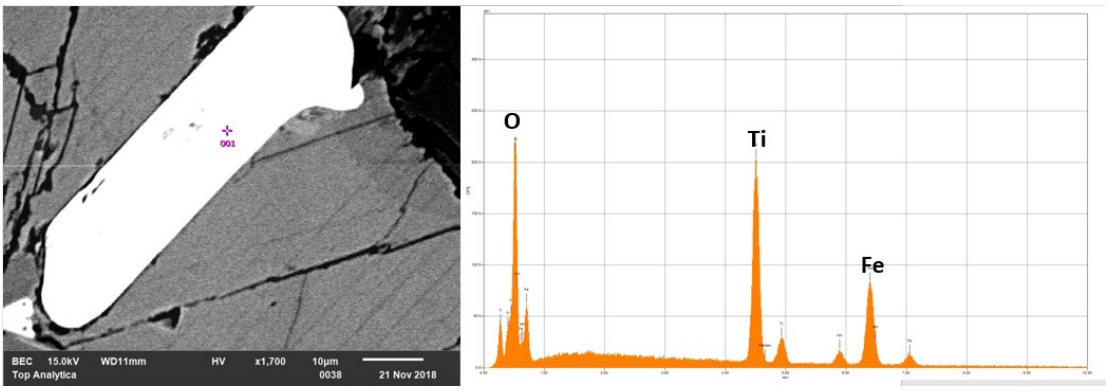

Figure 17. Ilmenite in thin section 015. EDS analysis point marked with a purple cross.

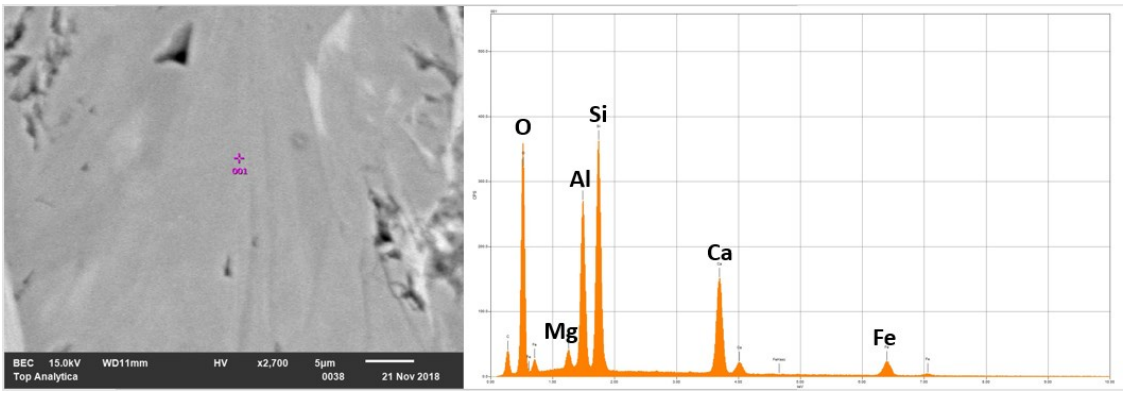

Figure 18. Pumpellyite in thin section 025. EDS analysis point marked with a purple cross.

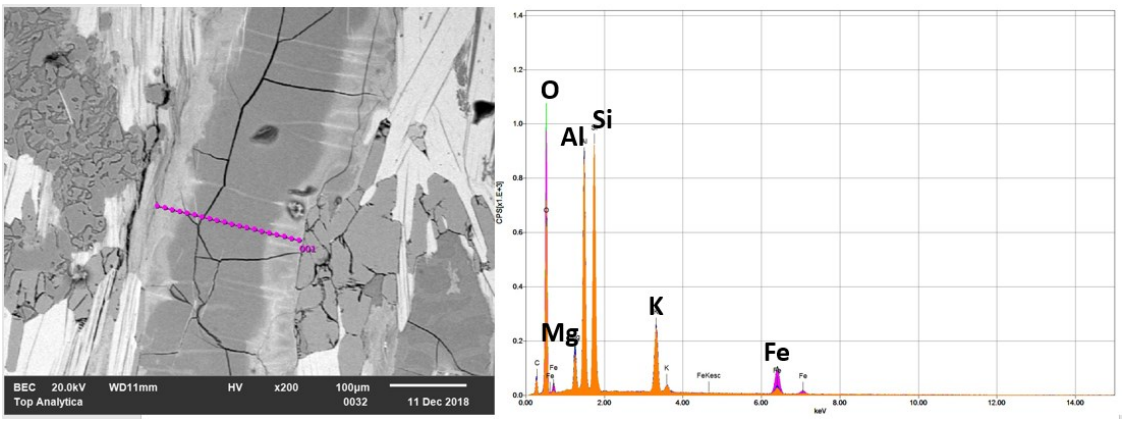

Figure 19. Line scan over unkown mineral in thin section 029, analyze spoints marked with purple dots. Increased iron concentration along grain borders due to iron oxide, assumed weathering product from surrounding rock.

6.4 Garnet-biotite thermometry

Four garnet-biotite pairs were analyzed with the Electron Micro-Probe in thin sections 29, 83, 113 and 177. The measurement points are seen as red dots (Figure 20). The calculations gave temperatures ranging from 505-640°C. Most calculations stay within 550°C ± 20°C (Figures 21 & 22).

Garnet and biotite compositions used for the calculations are seen in appendix D.

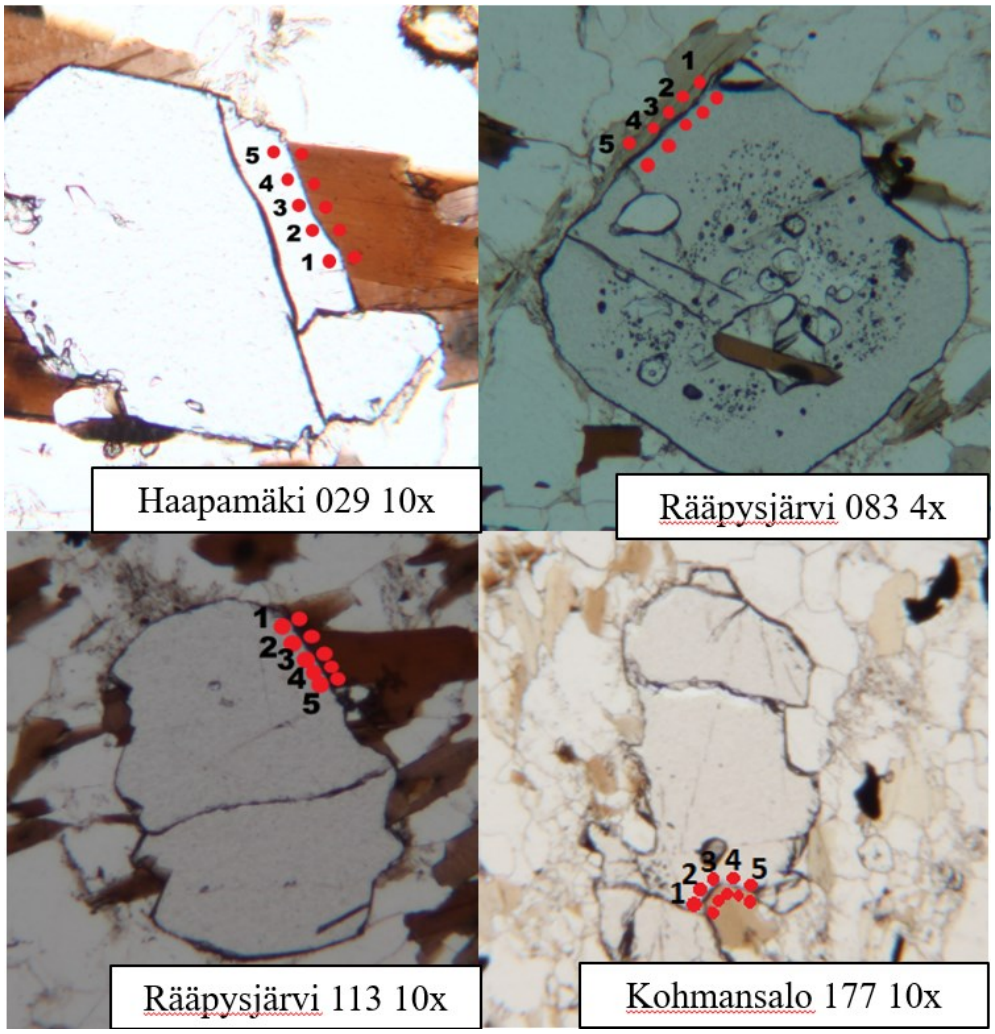

Figure 20. Garnet-biotite pairs from thin sections 29, 83, 113 and 177 in plane polarized view. Micro probe analyze points marked as numbered red dots.

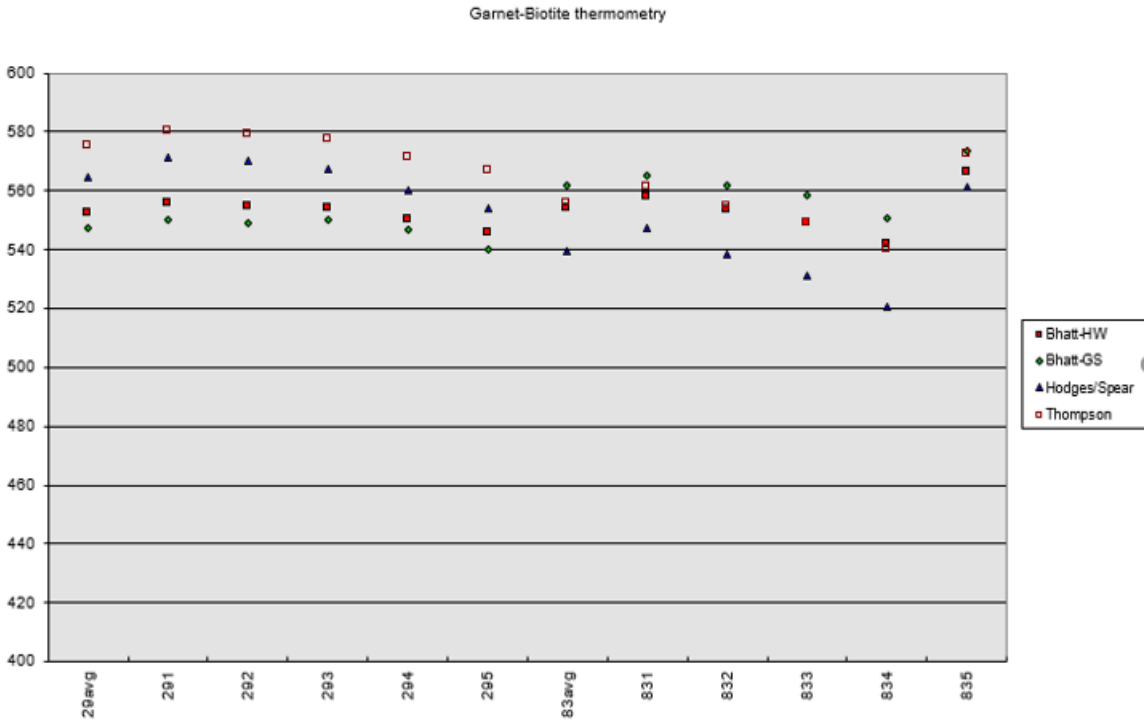

Figure 21. Graph of samples 29 and 83. Temperatures given for each point and average temperature.

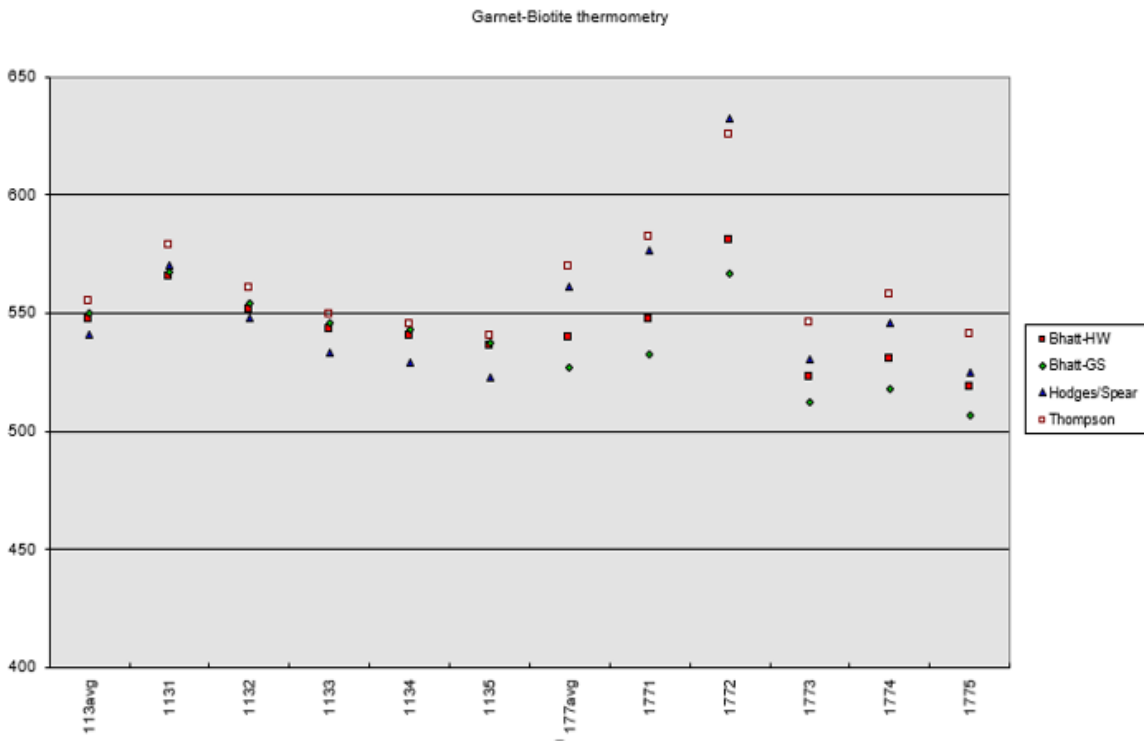

Figur 22. Graph of samples 113 and 177. Temperatures given for each point and average temperature.

6.5 Pseudosections

Chemical data that was used for the pseudosections can be seen in the appendix.

For pseudosection 083 a temperature range of 725 - 835°C was achieved. The mineral paragenesis of the rock include biotite, plagioclase, garnet and quartz (+ melt). The stability field can be seen in the center marked in red (Figure 23).

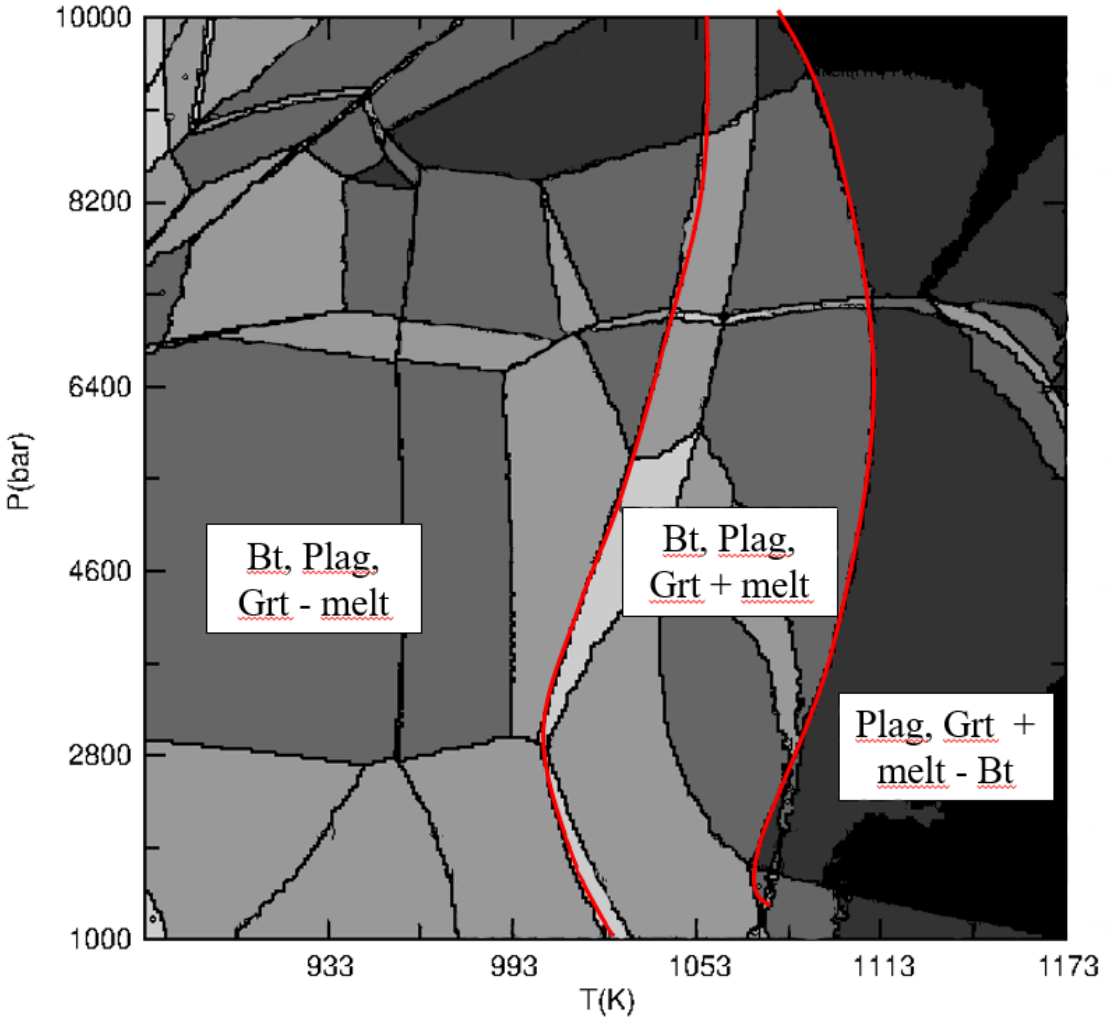

Figure 23. Pseudosection of sample 083. Stability field of the sample is marked in red, biotite is absent to the right and melt is absent to the left.

Pseudosection 015 has a narrower temperature range of 775-800 °C (Figure 24). Within the stability field are orthopyroxene, biotite, plagioclase, garnet, amphibole and ilmenite aswell as melt +- H_2O.

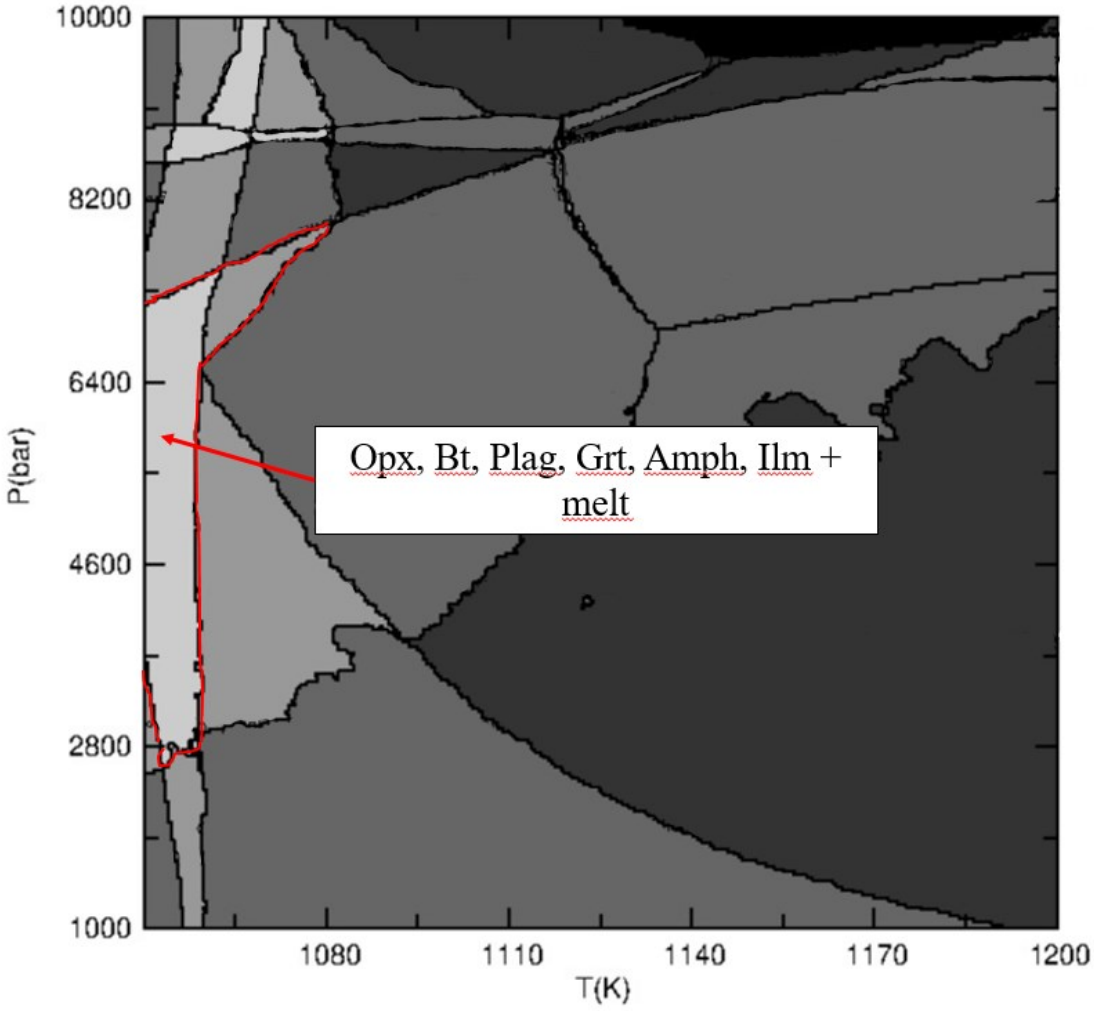

Figure 24. Pseudosection of sample 015. Stability field of the sample is marked in red.

Samples 166 and 177 did not yield any pseudosections.

7 Discussion

The purpose of this study is to determine the metamorphic degree of the Heinävesi area through field observations, petrographical observations, garnet-biotite thermometry and pseudosections. SEM was used to assist in mineral identification and micro probing.

Due to the existence of migmatites and orthopyroxene in the area a minimum temperature of 650-750 °C can be concluded, since migmatization of metapelites occurs at 650 °C and orthopyroxene has a minimum temperature of 750 °C in greywacke compositions (Hölttä & Heilimo 2017).

The temperatures gained from garnet-biotite thermometry are within a 505-640 °C range, which is too low to be considered peak temperature and is too low for partial melting. Field observations suggest a higher temperature than the max temperature gained through the thermometry.

The Raman-spectroscopy conducted by Iisa Witick in her thesis The Occurrence and Characterization of Graphitic Carbon in Southern Tuusniemi, South-Eastern Finland, 2017, also confirms, along with the field and petrohraphic observations, a higher peak temperature than the garnet-biotite thermometer suggests. In her work, due to the well-developed Raman pattern of the graphite, the thermometric calculations yield temperatures of 641 °C with the Beyssac et al. 2002 method and 737 °C with the Rahl et. al. 2005 method. Both are maximum temperatures of respective method, suggesting the real peak temperature is exceeding 737 °C.

The pseudosections show a temperature range of 725-835 °C and 775-800 °C. The second pseudosection from sample 015 has a narrower range compared to 083 and can be considered the more accurate one due to its more complex mineral paragenesis. Garnet, plagioclase and biotite has a wider stability field than orthopyroxene, biotite, plagioclase, garnet, amphibole and ilmenite.

The pressure and temperature ranges gained are of 775-800 °C and 2.8-8 kbar, suggesting upper amphibolite facies. According to Laajoki, et al. 2005 the Kainuu, Savo, Salahmi, Kiiminki and Kuopio supracrustal belts that are surrounding the investigated area are all within upper amphibolite facies supporting the results of this thesis.

On a larger scale, the upper Kaleva area shows a geographical variance in metamorphic degree as well. The metamorphic degree increases to the west and is lower to the east. Mineral assemblages from ultra-mafic bodies within the metasediments in the east include atg±ol±tr suggesting PT conditions of 500-550 C° and 3-5kbar. To the west temperatures of 725-775 C° with pressures of 3-5 kbar have been observed, with assemblages of ol-enst±ath±MgAl-spl, placing the western parts in upper-amphibolite facies (Hölttä & Heilimo, 2017) which supports the results of this thesis as well.

The pressure and temperature conditions gained from respective methods can be seen in Table 5 and 6.

Table 5. Temperatures gained from respective methods.

Method	Temperature Range (°C)
Field observations	>650
Petrography	>750
Grt-Bt Thermometry	505-640
Pseudosections	775-800
Witicks Ramanspectrometry	>737

Table 6. Pressures gained from respective methods.

Methods	Pressure range (kBar)
Petrography	0-9 kbar
Pseudosections	2.8-8 kbar

7.1 Garnet-biotite thermometric results

The temperatures gained by the garnet-biotite thermometry represent the temperature when the mineral pairs crystallized. It is possible that the crystallization of garnet and biotite occurred before the main metamorphic event. No zoning of the garnets was observed but some showed inclusion-rich centers while exhibiting inclusion-free rims. Continued growth of garnets during retrograde metamorphism is possible.

Other observed minerals and alterations such as sericitation, biotite dehydration, epidote and pumpellyite suggest retrograde metamorphic reactions or overprinting. Pumpelleyite indicates an anti-clockwise retrograde pressure and temperature path, peaking at upper amphibolite facies according to the pseudosection analysis, orthopyroxene and migmatite observations and Iisa Witick's raman spectroscopy, and abates toward sub-greenschist facies where the pumpellyite crystallized. In the transition from amphibolite to sub-greenschist facies, the garnets might have crystallized or grown

8 Conclusion

The rocks within the Heinävesi area are mostly biotite-quartz-plagioclase gneisses with varying graphite content ranging from disseminated flakes to several percentages. Diatexites and metatexites are common, indicating partial melting and orthopyroxene, garnet and amphibole-bearing layers occur sparsly. The quality of graphite is greatly influenced by the temperature conditions. A higher metamorphic degree enables higher quality graphite to crystallize with a more well-ordered crystal lattice.

The rocks in the area belong to the upper Kaleva tectonostratigraphic unit and were deposited in a marine basin created by the break-up of the Neoarchean continent during 2.1-2.05 Ga. During the Svecofennian orogeny when the microcontinent Keitele accreted at 1.91 Ga the sediments were metamorphosed, deformed and thrusted into complex allochtons. The metamorphic degree is in high amphibolite facies with a temperature range of 775-800 °C with pressures between 2.8 and 8 kbar (Figure 25) making the area suitable for further graphite exploration.

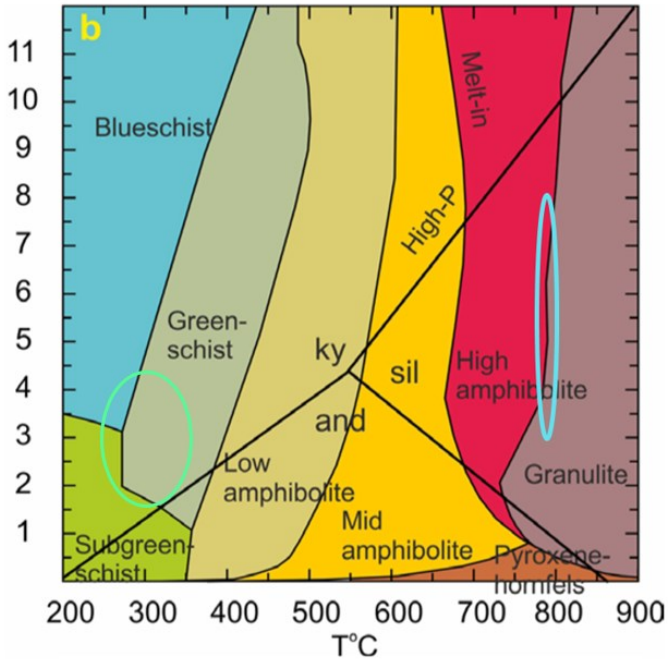

Figure 25. Diagram of the metamorphic facies. Study area marked with a light blue circle and pumpellyite facies with a light green circle (Hölttä & Heilimo 2017).

9 Acknowledgements

I want to thank my supervisors Professor Olav Eklund (Åbo Akademi) and Jenni Palosaari (Åbo Akademi) as well as the Beowulf Mining plc crew Rasmus Blomqvist (Exploration Manager) and Sauli Raunio (Geologist) for allowing me to be part of the Fennoflakes-project. I would also like to thank Sören Fröjdö (Åbo Akademi) for conducting the micro-XRF analysis and Casimir Näsi (Top Analytica Oy Ab) for handling the microprobe and SEM analyses.

10 Svensk sammanfattning – Swedish summary

Bestämning av metamorfosgraden hos grafitfyndigheter i Heinävesi-området

Introduktion

Metamorfos är en process där förändringar sker i berggrunden när den utsätts för förändrade tryck- och temperaturförhållanden. Grafitens kvalitet gynnas av hög metamorfosgrad och ur malmletningsperspektiv är det av intresse att veta metamorfosgraden hos grafitförekomster.

Metamorfosraden hos grafitfyndigheterna i Heinävesi-området har bedömts genom fältobservationer, pseudosektioner, biotit-granat-termometri och tunnslipsanalys.

Grafit är ett mineral varav enskilda kollager är bundna till varandra med svaga van-der-Vaals bindningar i ett hexagonalt nätverk. De enskilda kollagren kallas grafen och har goda el- och värmeledande egenskaper. På dessa grunder är grafen ett eftertraktat material med stor potential inom elektronikindustrin med möjliga högteknologiska tillämpningar som i avancerade datorer i olika former och i solpaneler (Olson 2012). Grafit används även för tillverkning av eldfasta material, pennor, bussningar, bränsleceller, smörjmedel med mera (Kogel et. Al. 2006). Efterfrågan på grafit ökar konstant och har upptagits på Europeiska unionens lista över kritiska råvaror (Europeiska kommissionen 2017).

För att producera varor, specifikt högteknologiska produkter, bör grafiten vara av god kvalitet och ha ett välutvecklat kristallgitter. Kvaliteten är kraftigt bunden till temperaturen under kristallisationsförloppet. I områden med hög metamorfosgrad kan grafit av hög kvalitet förväntas.

Geologisk bakgrund

Studieområdet ligger i övre Kaleva tektofacies i östra Finland i Heinävesi. Bergarten består i huvudsak av peliter, psammiter och gråvackor som deponerades i en djuphavsbassäng kring 1,939–1,942 Ga. Bassängen bildades när den neoarkeiska kontinenten delades vid 2,1–2,05 Ga (Niironen 2017). Sedimentationen fortgick tills det huvudsakliga kollisionsskedet under den svekofenniska orogenin vid tiden 1,92–1,87 Ga (Laajoki et al. 2005). Vid 1,91 Ga, då mikrokontinenten Keitele anhopades, metamorfoserades Kaleva sedimenten (Niironen 2017). Graden av metamorfosen undersöks i denna avhandling.

Material och metoder

Materialet i denna avhandling består av 180 fältobservationer och 80 prover. Proverna valdes utgående från grafithalt och avvikande mineralogiska egenskaper i jämförelse med omgivande berggrund.

Pseudosektioner och granat-biotit-termometri utfördes för tryck- och temperaturbedömning. För pseudosektioner krävs bulkkemisk analys och mineralogiska observationer, som matas in i programvaran Perple_X som producerar diagram med stabilitetsfält som olika mineralogiska sammansättningar. Den bulkkemiska analysen för pseudosektionerna utfördes med röntgenfluorescensanalys (XRF) och de mineralogiska observationerna genom mikroskopering av tunnslip med korspolariserat mikroskop. Kunde inte mineralen identifieras med mikroskop användes svepelektronmikroskop (SEM).

För granat-biotit-termometrin utfördes elektronsondmikroanalys vid korngränserna. Skillnaden i den kemiska sammansättningen mellan mineralen användes för temperaturberäkning. Tabeller över elementen som användes i beräkningarna kan ses i appendix D.

Resultat

Granat-biotit-termometrin resulterade i temperaturer under 650 °C medan resterande metoder i temperaturer över 650 °C, vilket tyder att granat-biotit-termometrin är en opassande metod för bedömning av metamorfosgraden i detta område. Observerade metatexiter och diatextiter i fält anger en temperatur på 650 °C och tunnslipsobservationer en minimitemperatur på 750 °C. Pseudosektionerna placerar området i ett temperaturintervall på 725–835 °C och 775–800 °C och ett tryckintervall på 2,8–8 kbar. Enligt ramanspektrometrin utförd av Witick, I. 2017 på grafitflak från området bekräftas maximitemperaturen ligga ovanför 737 °C (Tabell 1).

Tabell 1. Temperaturer enligt respektive analysmetod.

Metod	Temperatur (°C)
Fältobservationer	>650
Tunnslip	>750
Grt-Bt Termometri	505–640
Pseudosektioner	775–800
Witicks Ramanspektrometri	>737

Diskussion

Målet med studien är att bestämma metamorfosgraden för området genom fält- och mineralogiska observationer, granat-biotit termometri och pseudosektioner.

Fält- och mineralogiska observationer resulterar i temperaturer från 650 °C till över 750 °C. Minimitemperaturen för migmatiseringen av metapeliter är 650 °C. Den lägsta stabilitetstemperaturen för ortopyroxen i metapelitisk sammansättning är 750 °C (Hölttä & Heilimo 2017). Eftersom migmatiter och ortopyroxen har identifierats, både i fält och tunnslip, motstrids temperaturen angiven av granat-biotit-termometrin. Granat-biotit-ermometrin anger temperaturen då kristallparen kristalliserades, vilket antagligen är före metamorfosens kulmen och kan inte anses som representativ för metamorfosgraden.

Pseudosektion 015 resulterade i ett temperaturintervall på 775–800 °C som reflekterar maximitemperaturen i området bäst. Den mineralogiska sammansättningen för 015 är ortopyroxen, biotit, plagioklas, granat, amfibol, ilmenit och smälta. Pseudosektion 083 uppvisade ett bredare temperaturintervall på 725–835 °C och bestod av mindre varierad mineralogisk sammansättning än 015. Mineralena för 083 är biotit, plagioklas, granat och smälta.

I tunnslip och SEM-analyser identifierades pumpellit, ett låg metamorft mineral, som tyder på retrograd metamorfos i pumpellitfacies efter huvudmetamorfosskedet.

Slutsats

Bergarten i Heinävesi-området är i huvudsak biotit-kvarts-plagioklas-gneiss med varierande grafithalt från enskilda disseminerade flak till flera procent grafit. Bergarten metamorfoserades vid kollisionen med Keitele mikrokontinenten vid 1,91 Ga. Tryck- och temperaturförhållanden under metamorfosen ligger mellan 775–800 °C och 2,8–8 kbar. Detta placerar området i övre amfibolitfacies och gränsar granulitfacies (Figur 1). Den höga metamorfosgraden gör området lämpligt för malmletning av grafit.

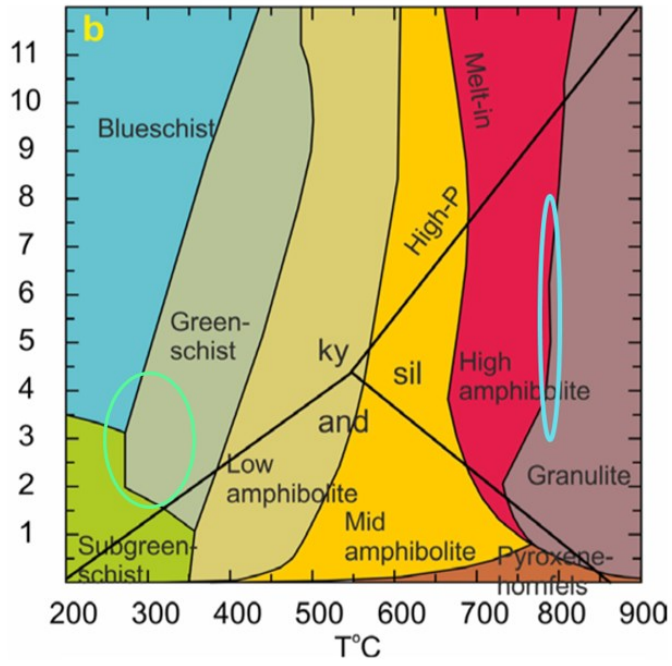

Figur 1. Tryckt och temperaturdiagram med metamorfosfacies. Blåa ringen representerar studieområdet och gröna pumpellitfacies (Hölttä & Heilimo 2017).

11 References

Ahtola, T., Kuusela, J. 2015. Esiselvitys Suomen grafiittipotentiaalista. Geologian tutkimuskeskus (GTK). Report 88/2015. 14 p.

Behrends, T & Kleingeld, P., 1.2009. Bench-top micro-XRF – a useful apparatus for geochemists? [https://www.geochemsoc.org/publications/geochemicalnews/gn138jan09/benchtopmicroxrfausefulapp]. Accessed 19.2.2019

Brady, J & Perkins, D., 17.1.2019. Mineral Formulae Recalculation. Smith College & University of North Dakota [https://serc.carleton.edu/research_education/equilibria/mineralformulaerecalculation.html]. Accessed 22.2.2019

European commission 2017. *Critical Raw Materials* [http://ec.europa.eu/growth/sectors/raw-materials/specific-interest/critical_en]. Accessed 31.10.2018

European commission 2017. *Communication on the list of Critical Raw Materials* [https://eur-lex.europa.eu/legal-content/EN/TXT/?uri=CELEX:52017DC0490]. Accessed 31.10.2018

Goodge, J., 16.5.2017. Electron probe micro-analyzer (EPMA). University of Minnesota-Duluth [https://serc.carleton.edu/research_education/geochemsheets/techniques/EPMA.html]. Accessed 8.2.2019.

Hazen, R.M., Downs, R.T., Jones, A.Poch Kah, L., 2013. Carbon Mineralogy and Crystal Chemistry. Hazen, R.M., Jones, A.P. och Baross, J.A. (eds) Carbon in Earth. Reviews in Mineralogy & Geochemistry, 75. Mineralogical Society of America, Chantilly, Virginia. pp.7-46.

Henry, D., 10.11.2016. Electron-sample Interactions Louisiana State University. [https://serc.carleton.edu/research_education/geochemsheets/electroninteractions.html]. Accessed 11.2.2019

Hirsch, D & Baldwin, J., 10.11.2016. Advanced Modeling Programs: Perplex. Western Washington University. [https://serc.carleton.edu/research_education/equilibria/perplex.html]. Accessed 20.2.2019

Hirsch, D., Baldwin, J., Perkins, D., 11.10.2016. Pseudosections. Western Washington University, University of Montana, University of North Dakota. [https://serc.carleton.edu/research_education/equilibria/pseudosections.html]. Accessed 12.2.2019

Hölttä, P & Heilimo, E. 2017. Metamorphic Map of Finland. Geological survey of Finland. Special paper 60, pp. 77-128.

Laajoki, K., Lehtinen, M., Nurmi, P.A., Rämö, O.T., 2005, Precambrian Geology of Finland – Key to the Evolution of the Fennoscandian Shield. Elsevier B.V., Amsterdam, pp. 279–342

Landis, C.A., 1971. Graphitization of Dispersed Carbonaceous Material in Metamorphic Rocks. Contributions to Mineralogy and Petrology, 30. 34-45.

Luukas, J et. al. 2017. Major Stratigraphic Units in the Bedrock of Finland, and an approach to Tectonostratigraphic Division. Geological survey of Finland. Special paper 60, pp. 9-40.

Kogel, J.E., Trivedi, N.C., Barker, J.M., Krukowski, S.T., 2006, Industrial Minerals & Rocks. Society for Mining, Metallurgy, and Exploration, Inc, pp. 507-518.

Molina, J.F., Moreno, J.A., Castro, A., Rodríguez, C., Fershtater, G.B., 2015. Calcic amphibole thermobarometry in metamorphic and igneous rocks: New calibrations based on plagioclase/amphibole Al-Si partitioning and amphibole/liquid Mg partitioning. Elsevier. Volume 232. pp. 286-305.

Nabighian, M.N., 1991. Investigations in Geophysics. Electromagnetic Methods in Applied Geophysics: Pars A and B. Volume 2 p. 967.

Nesse, W.D., 2004, Introduction to optical mineralogy Third edition, Oxford University Press Inc., 348 pp.

Nironen, M. 2017. Guide to the Geological Map of Finland – Bedrock 1:1 000 000. Geological survey of Finland. Special paper 60, pp. 41-76.

Olson, D.W., 2012, Graphite [advance release] in 2012 Minerals Yearbook by U.S. Geological Survey.

Pierson, H.O., 1993, Handbook of carbon, graphite, diamond and fullerenes. Noyes Publications, New Jersey. 399 p.

Swapp, Susan. 26.5.2017. Scanning Electron Microscopy (SEM). University of Wyoming. [https://serc.carleton.edu/research_education/geochemsheets/techniques/SEM.html]. Accessed 11.2.2019

University Of Oxford, Earth Sciences. 12.10.2004. Practical Aspects of Mineral Thermobarometry. [https://www.earth.ox.ac.uk/~davewa/pt/pt-start.html]. Accessed 22.2.2019.

Vaasjoki, M., Korsman, K., Koistinen, T., 2005, Precambrian Geology of Finland – Key to the Evolution of the Fennoscandian Shield. Elsevier B.V., Amsterdam, pp. 1–18.

Wirth, K., & Barth, A., 17.2.2019. X-Ray Fluorescence (XRF). Macalester College, Indiana university-Purdue University, Indianapolis [https://serc.carleton.edu/research_education/geochemsheets/techniques/XRF.html]. Accessed 19.2.2019.

Witick, I. 2017. The Occurrence and Characterization of Graphitic Carbon in Southern Tuusniemi, South-Eastern Finland. Master's thesis. Åbo Akademi University. 49 p.

Appendix

Appendix A

Field observation, observation ID, coordinates, sample, rock type, texture, ore minerals, ore style, ore percentage, foliation and field notes.

OBS_ID	PROSPECT	EASTING	NORTHING	DATE	SAMPLE	ROCK TYPE	TEXTURE	Ore minerals	Ore min style/size	Ore min %	FOLIATION DD	FOL DIP	FIELD_NOTES
2017-ME-001	Haapamäki	3572227	6940997	15.5.2017	Yes	QFB gneiss	foliated, banded				198	60	thin quartz veins along foliation, strong aeromag anomaly
2017-ME-002	Haapamäki	3572319	6941164	15.5.2017	Yes	Garnet bearing QFB gneiss	foliated, banded				204	72	at site deformed, irregular folding, DD/Dip varies on site (185/70, 204/72, 240/74), large garnets in mafic parts (up to 2mm). Fold axis 260/69
2017-ME-003	Haapamäki	3572100	6941246	15.5.2017	Yes	Garnet bearing QFB gneiss	foliated, banded	graphite	disseminated, patchy, 2mm flakes	1 %	204	68	slightly rusty, quartz veins along foliation, alternating slightly softer mica layers with graphite up to 2% , graphite interlayered with biotite with flake

													size of 2mm, sulfide stringers 2%
2017-ME-004	Haapamäki	3572064	6941010	15.5.2017	Yes	Graphite schist	strong foliation	graphite	disseminated, semi massive in places	6-8%	194	80	structures measured 10m west from site, 40m east of site rock turns more granitic with mafic flames, pegmatite vein with sharp contact with metasediment 224/64?
2017-ME-005	Haapamäki	3571899	6941075	15.5.2017	No	QFB gneiss	moderate foliation, banded				186	62	slightly boudinaged, quartz veins along foliation, around site alternating pegmatitic layers
2017-ME-006	Haapamäki	3571872	6941340	15.5.2017	Yes	QFB gneiss	moderate foliation	graphite	1mm flakes in mafic parts	<1%	206	66	1mm graphite flakes, graphite in mafic parts
2017-ME-007	Haapamäki	3571636	6941245	15.5.2017	Yes	QFB gneiss	foliated, homogenous	graphite	disseminated	1-2%	184	64	rusty and weathered on surface, homogenous, few leukosomes
2017-ME-008	Haapamäki	3571644	6941360	15.5.2017	Yes	Graphite schist	strong foliation	graphite	disseminated, partly enriched in patches	6-8%	158	70	host rock QFB gneiss, graphite schist layers 5-10cm thick
2017-ME-009	Haapamäki	3571210	6941453	16.52.017	No	QFB gneiss	strong to moderate foliation				184	78	thick granitic layers 0.5m in gneiss, strong aeromag anomaly, 60m W

													same rock, soft weathered mafic parts
2017-ME-010	Haapamäki	3571113	6941470	16.5.2017	Yes	Migmatitic granite	weak foliation				182	78	30% of site consist of intermediate volcanite (IMV)?, IMV weak foliation, undisturbed, dark, homogenous with sharp contact to migmatitic granite along foliation, strong aeromag anomaly
2017-ME-011	Haapamäki	3571038	6941428	16.5.2017	No	QFB gneiss	slightly migmatitic, foliated, banded	graphite	disseminated	<1%	196	68	graphite in mafic parts of granite, strong aeromag anomaly
2017-ME-012	Haapamäki	3571157	6941679	16.5.2017	Yes	QFB gneiss	moderate foliation				204	72	rusty, contains sulfides, quartz veins along foliation, slightly deformed, strong aeromag anomaly
2017-ME-013	Haapamäki	3570826	6941497	16.5.2017	No	QFB gneiss	moderate foliation				200	68	red quartz veins along foliation, same rock 50m S of site, slightly rusty, strong aeromag anomaly
2017-ME-014	Haapamäki	3570735	6941519	16.5.2017	No	Vein quartz							quartz varies in color between red brown and milky white, diffuse

													contact with side rock QFB gneiss
2017-ME-015	Haapamäki	3570373	6941575	16.5.2017	Yes	QFB gneiss	moderate foliation	graphite	traces	<1%	208	68	360m E of site same rock, slightly rusty, large mica flakes in mica rich layers, biotite and muscovite, flake size up to 1cm, strong aeromag anomaly
2017-ME-016	Haapamäki	3570382	6941792	16.5.2017	Yes	Tonalite?	massive, mineral lineation, homogenous						massive, homogenous, even grained tonalite?, pale or almost white, 228/62 lineation
2017-ME-017	Haapamäki	3570436	6941815	16.5.2017	No	QFB gneiss	moderate foliation, banded				198	74	tonalite vein cuts QFB gneiss 90 degrees against foliation, the tonalite has a mineral lineation of 228/62 and is similar as in site 016
2017-ME-018	Haapamäki	3570699	6941641	16.5.2017	Yes	QFB gneiss	moderate foliation, homogenous	graphite	disseminated, fine grained 0.1-0.5mm	<1%	190	74	~2% sulfide content, assymetric sinistral fold with ptygmatic folds in more felsic layers
2017-ME-019	Haapamäki	3570898	6941672	16.5.2017	No	QFB gneiss	moderate foliation				194	72	quartz veins along foliation, 100m E of

													site same rock, slightly rusty
2017-ME-020	Haapamäki	3570926	6941785	16.5.2017	No	QFB gneiss	moderate foliation, banded				218	64	slightly rusty, edge of aeromag anomaly
2017-ME-021	Haapamäki	3570735	6942091	16.5.2017	Yes	QFB gneiss	moderate foliation				196	70	boudinage, weak aeromag anomaly
2017-ME-022	Haapamäki	3570590	6941918	16.5.2017	No	QFB gneiss	moderate foliation	graphite	traces, coarse flakes up to 2mm	<1%	202	64	quartz veins along foliation, strong aeromag anomaly
2017-ME-023	Haapamäki	3570260	6941797	17.5.2017	Yes	QFB gneiss	moderate foliation	graphite	disseminated	1 %	194	76	slightly rusty, 0.5m granitic vein cuts gneiss 90 degrees against foliation, contact 290/80, granite is massive and medium grained, strong aeromag anomaly
2017-ME-024	Haapamäki	3570135	6941699	17.5.2017	No	QFB gneiss	moderate foliation	graphite	traces of graphite in mica rich layers	<1%	178	78	150m NE of site same rock, boudinage, strong aeromag anomaly, (IN PICTURE CHALK BOARD SAYS 023 NOT 024, hammer points to lover left corner in picture)
2017-ME-025	Haapamäki	3570086	6941523	17.5.2017	Yes	QFB gneiss	moderate foliation				182	70	slightly rusty, slightly deformed, strong aeromag anomaly

2017-ME-026	Haapamäki	3570058	6941476	17.5.2017	No	QFB gneiss	moderate foliation				192	64	quartz veins along foliation, weak aeromag anomaly
2017-ME-027	Haapamäki	3569930	6941555	17.5.2017	No	QFB gneiss	moderate foliation, migmatitic	graphite	traces of graphite, disseminated, flakes up to 2mm in granitic parts	<1%	180	68	weak aeromag anomaly
2017-ME-028	Haapamäki	3569883	6941723	17.5.2017	Yes	QFB gneiss	moderate foliation, migmatitic, deformed				198	70	quartz veins along foliation, 100m N of site same rock
2017-ME-029	Haapamäki	3569994	6941893	17.5.2017	Yes	Garnet bearing QFB gneiss	moderate foliation, migmatitic				204	78	visible garnets in paleosome, slightly rusty, moderate aeromag anomaly
2017-ME-030	Haapamäki	3569998	6942023	17.05.2017	No	QFB gneiss	moderate foliation, migmatitic				188	70	quartz veins along foliation
2017-ME-031	Haapamäki	3570276	6941993	17.05.2017	No	QFB gneiss	moderate foliation				194	60	slightly rusty
2017-ME-032	haapamäki	3570130	6942214	17.05.2017	No	QFB gneiss	moderate foliation				188	70	quartz veins along foliation, low aeromag anomaly
2017-ME-033	Haapamäki	3569580	6942183	17.05.2017	No	QFB gneiss	moderate foliation				174	72	boudinage
2017-ME-034	Haapamäki	3569755	6942062	17.05.2017	No	QFB gneiss	moderate foliation				182	68	moderate aeromag anomaly
2017-ME-035	Haapamäki	3569655	6941814	17.05.2017	Yes	QFB gneiss	moderate foliation, migmatitic				172	78	quartz veins along foliation, strong aeromag anomaly
2017-ME-036	Haapamäki	3569329	6941721	17.05.2017	No	QFB gneiss	moderate foliation, deformed				186	68	slightly rusty, stron aeromag anomaly

2017-ME-037	Haapamäki	3569221	6942046	17.05.2017	No	QFB gneiss	moderate foliation				174	88	moderate aeromag anomaly
2017-ME-038	Haapamäki	3569177	6941645	19.05.2017	No	QFB gneiss	weak foliation, homogenous				160	80	quartz veins along foliation, strong aeromag anomaly
2017-ME-039	Haapamäki	3569457	6941495	19.05.2017	Yes	QFB gneiss	moderate foliation, migmatitic, very deformed				188	78	slightly rusty, 100m W of site same rock, weak aeromag anomaly
2017-ME-040	Haapamäki	3568874	6941586	19.05.2017	Yes	QFB gneiss	moderate foliation	graphite	disseminated, 1-2mm flakes	<1%	190	70	quartz veins along foliation, strong aeromag anomaly
2017-ME-041	Haapamäki	3568924	6941802	19.05.2017	No	QFB gneiss	moderate foliation, banded, migmatitic				170	86	slightly rusty, strong aeromag anomaly
2017-ME-042	Haapamäki	3568872	6942088	19.05.2017	Yes	QFB gneiss	moderate foliation, banded	graphite	traces of graphite in mica rich layers, disseminated	<1%	196	70	strong aeromag anomaly
2017-ME-043	Haapamäki	3569074	6942264	19.05.2017	No	QFB gneiss	moderate foliation, slightly deformed						strong aeromag anomaly
2017-ME-044	Haapamäki	3569260	6942235	19.05.2017	Yes	QFB gneiss	moderate foliation	graphite	disseminated, patchy	<1%			slightly rusty, weathered, strong aeromag anomaly
2017-ME-045	Haapamäki	3569468	6942372	19.05.2017	No	QFB gneiss	moderate foliation				184	70	moderate aeromag anomaly
2017-ME-046	Haapamäki	3569161	6942463	19.05.2017	No	QFB gneiss	moderate foliation, migmatitic				178	72	no aeromag anomaly

2017-ME-047	Haapamäki	3568746	6942284	19.05.2017	Yes	QFB gneiss	moderate foliation				226	70	quartz veins along foliation, strong aeromag anomaly
2017-ME-048	Haapamäki	3568447	6942341	19.05.2017	Yes	Garnet bearing QFB gneiss	moderate foliation				192	74	garnet bearing, strong aeromag anomaly
2017-ME-049	Haapamäki	3568188	6942224	19.05.2017	No	QFB gneiss	moderate foliation				178	68	slightly rusty, strong aeromag anomaly
2017-ME-050	Haapamäki	3567730	6942089	19.5.2017	No	QFB gneiss	moderate foliation				180	60	quartz veins along foliation
2017-ME-051	Haapamäki	3568612	6941726	20.5.2017	No	QFB gneiss	moderate foliation, banded				180	70	250m W of site same rock, moderate aeromag anomaly
2017-ME-052	Haapamäki	3568195	6941840	20.5.2017	Yes	QFB gneiss	moderate foliation, migmatitic, deformed	graphite	traces of graphite, disseminated, 1mm flakes	<1%	155	88	weak to no aeromag anomaly, foliation difficult to measure due to deformation
2017-ME-053	Haapamäki	3567980	6941580	20.5.2017	Yes	QFB gneiss	moderate foliation, banded	graphite	disseminated, patchy, occurs in mica rich granitic layers, up to 1mm flakes	<1%	170	84	moderate aeromag anomaly
2017-ME-054	Haapamäki	3567755	6941455	20.5.2017	No	QFB gneiss	moderate foliation				190	80	quartz veins along foliation
2017-ME-055	Haapamäki	3567608	6941423	20.5.2017	Yes	Intermediate volcanite?	weak foliation, homogenous				310	70	small cutting granite veins moderate aeromag anomaly, weak foliation difficult to measure

2017-ME-056	Haapamäki	3567611	6941224	20.5.2017	No	QFB gneiss	moderate foliation, banded, migmatitic				150	80	moderate aeromag anomaly
2017-ME-057	Haapamäki	3567768	6941288	20.5.2017	Yes	QFB gneiss	weak foliation, migmatitic	graphite	disseminated, patchy, 1mm flakes	<1%	160	72	very weathered and rusty, contains sulfides, strong aeromag anomaly
2017-ME-058	Haapamäki	3567957	6941295	20.5.2017	No	QFB gneiss	moderate foliation, migmatitic				174	72	slightly rusty, 250m NE same rock, moderate aeromag anomaly
2017-ME-059	Haapamäki	3568247	6941427	20.5.2017	No	QFB gneiss	weak foliation, migmatitic, deformed				170	70	strong aeromag anomaly
2017-ME-060	Haapamäki	3568432	6941529	20.5.2017	No	QFB gneiss	moderate foliation				192	64	strong aeromag anomaly
2017-ME-061	Haapamäki	3568566	6941436	20.5.2017	No	QFB gneiss	moderate foliation, banded, migmatitic				192	60	strong aeromag anomaly
2017-ME-062	Haapamäki	3568627	6941615	20.5.2017	No	QFB gneiss	moderate foliation, homogenous				170	80	quartz clusters
2017-ME-063	Haapamäki	3567500	6942147	21.5.2017	No	QFB gneiss	moderate foliation, slightly migmatitic				350	88	large coarse leucosome, quartz veins along foliation, weak aeromag anomaly
2017-ME-064	Haapamäki	3568208	6942020	21.5.2017	No	Migmatitic granite	massive						mafic flames in granite, foliation of the flames follow the common trend

													in the area, weak to no aeromag anomaly
2017-ME-065	Haapamäki	3567808	6941902	21.5.2017	Yes	QFB gneiss	moderate foliation, slightly deformed	graphite	disseminated, patchy, 1-2mm flakes	<1%	180	90	no aeromag anomaly
2017-ME-066	Haapamäki	3567306	6941379	21.5.2017	No	QFB gneiss	moderate foliation				308	88	quartz veins along foliation, weak aeromag anomaly
2017-ME-067	Haapamäki	3567359	6941790	21.5.2017	No	QFB gneiss	migmatitic, very deformed						foliation of mafic parts follow common trend, slighlty rusty, rock disturbs compass, moderate aeromag anomaly
2017-ME-068	Rääpysjärvi	3575435	6946447	6.6.2017	No	QFB gneiss	moderate foliation				300	72	weak aeroEM anomaly
2017-ME-069	Rääpysjärvi	3575362	6946140	6.6.2017	Yes	Garnet bearing QFB gneiss	weak to moderate foliation, homogenous				348	72	few granitic parts, garnets <1mm big, no aeroEM anomaly
2017-ME-070	Rääpysjärvi	3575314	6946100	6.6.2017	Yes	Graphite schist	moderate foliation	graphite	enriched in patches with flakes up to 4mm, disseminated graphite in side rock	~5%			extremely weathered, rusty and sulfidic, very soft and brittle, no aeroEM anomaly
2017-ME-071	Rääpysjärvi	3575147	6945990	6.6.2017	No	QFB gneiss	moderate foliation, very deformed						very deformed gneiss all around the hill, foliation not properly measurable, weak

													to no aeroEM anomaly
2017-ME-072	Rääpysjärvi	3575265	6945744	6.6.2017	No	QFB gneiss	moderate foliation, deformed				262	72	200m NNE same rock, moderate aeroEM anomaly
2017-ME-073	Rääpysjärvi	3575371	6946049	6.6.2017	No	QFB gneiss	moderate foliation, homogenous				338	76	aplitic granite vein cuts foliation at 40 degrees, vein has no mafic minerals and is fine grained at borders and coarses in the middle, no aeroEM anomaly
2017-ME-074	Rääpysjärvi	3575488	6945957	6.6.2017	Yes	QFB gneiss/Graphite schist	moderate foliation	graphite	disseminated, patchy, 1-2mm flakes	2-5%			extremely weathered, rusty, sulfidic and brittle, graphite schist occur at some boulders
2017-ME-075	Rääpysjärvi	3575561	6945978	7.6.2017	No	QFB gneiss	moderate foliation				322	68	quartz veins along foliation, no aeroEM anomaly
2017-ME-076	Rääpysjärvi	3576327	6946137	07.06.2017	No	QFB gneiss	moderate foliation, banded, very deformed				230	80	no aeroEM anomaly, whole area around observation (hiekkalahdenmäki) very poorly exposed
2017-ME-077	Rääpysjärvi	3576357	6945513	07.06.2017	Yes	Graphite schist	moderate foliation, very deformed	graphite	graphite in mica (biotite) rich layers, flake size 2-3mm	2-3%	320	80	weathered, rusty, sulfidic, brittle, coarse grained quartz clusters,

													granitic veins with ptygmatic folds on outcrops close to observation (60m W), weak aeroEM anomaly
2017-ME-078	Rääpysjärvi	3576088	6945736	07.06.2017	No	QFB gneiss	weak to moderate foliation	graphite	traces of graphite in mica rich layers	<1%			moderate to strong aeroEM anomaly
2017-ME-079	Rääpysjärvi	3575819	6945642	07.06.2017	Yes	Garnet bearing QFB gneiss	moderate foliation, slightly deformed				334	72	granitic parts folded in sinistral assymetric folds, moderate to strong aeroEM anomaly
2017-ME-080	Rääpysjärvi	3576557	6945419	07.06.2017	Yes	Graphite schist	weak foliation	graphite	graphite in mica (biotite) rich layers, patchy and enriched in certain areas, flake size 2-3mm	3-4%			extremely weathered, rusty, sulfidic and brittle, not very soft, multiple graphite schist boulders in the area, another ~40m SSE along forest road, stron aeroEM anomaly
2017-ME-081	Rääpysjärvi	3576522	6945291	07.06.2017	No	QFB gneiss	moderate foliation, slightly deformed				248	72	200m W same rock, weak aeroEM anomaly
2017-ME-082	Rääpysjärvi	3576414	6945005	08.06.2017	No	QFB gneiss	moderate foliation						magnetic anomaly very poorly exposed, strong aeroEM anomaly
2017-ME-083	Rääpysjärvi	3576988	6944947	08.06.2017	Yes	Garnet bearing QFB gneiss	weak foliation				230	42	foliation difficult to measure properly,

													tight granitic ptygmatic folds, 130m N same rock, no aeroEM anomaly
2017-ME-084	Rääpysjärvi	3577072	6945208	08.06.2017	No	QFB gneiss	moderate foliation	graphite	traces of graphite	<1%			rusty, sulfidic, strong aeroEM
2017-ME-085	Rääpysjärvi	3577061	6945229	08.06.2017	Yes	Graphite schist	strong foliation	graphite	disseminated, flake size ~1mm	3 %			rusty, sulfidic, very brittle, several other graphite schist boulders 80m NE, strong aeroEM anomaly
2017-ME-086	Rääpysjärvi	3577126	6945261	08.06.2017	No	QFB gneiss	weak to moderate foliation						slightly rusty, moderate to strong aeroEM anomaly
2017-ME-087	Rääpysjärvi	3577263	6945150	08.06.2017	Yes	Graphite schist	moderate foliation	graphite	disseminated, patchy, flake size ~1mm	2 %			very rusty, sulfidic, brittle, many graphite schist boulders along creek bank, no aeroEM anomaly
2017-ME-088	Rääpysjärvi	3576627	6946301	08.06.2017	No	QFB gneiss	moderate foliation				172	82	slightly rusty, weak to no aeroEM anomaly
2017-ME-089	Rääpysjärvi	3577105	6945966	08.06.2017	Yes	QFB gneiss	moderate foliation, slightly deformed	graphite	traces of graphite, disseminated in mica rich parts	1 %	280	70	slightly rusty, strong aeroEM anomaly
2017-ME-090	Rääpysjärvi	3577170	6945935	08.06.2017	Yes	Graphite schist	weak to moderate foliation	graphite	disseminated and patchy, flake size up to 3mm	3 %	348	78	rusty and sulfidic, strong aeroEM anomaly

2017-ME-091	Rääpysjärvi	3577420	6945320	09.06.2017	Yes	Graphite schist	moderate foliation	graphite	disseminated in groundmass, flake size 1mm,	5 %			rusty, sulfidic, brittle, many graphite schist boulders in the area, fine grained ground mass with large mica flakes up to 5mm, no aeroEM anomaly
2017-ME-092	Rääpysjärvi	3577150	6945449	09.06.2017	No	QFB gneiss	moderate foliation	graphite	traces of graphite, disseminated	<1%			no aeroEM anomaly
2017-ME-093	Rääpysjärvi	3577468	6945679	09.06.2017	No	Garnet bearing QFB gneiss	moderate foliation						no outcrops in the area only boulders, no aeroEM anomaly
2017-ME-094	Rääpysjärvi	3578066	6945332	09.06.2017	No	QFB gneiss	moderate foliation				310	88	large coarse grained quartz cluster, slightly rusty, no aeroEM anomaly
2017-ME-095	Rääpysjärvi	3578350	6945033	09.06.2017	Yes	Migmatitic granite	massive				350	80	mafic flames in granite, at places migmatitic QFB gneiss, flames and gneiss have a foliatioin around 350/80 but most of the outcrop consist of massive granite, no aeroEM anomaly
2017-ME-096	Rääpysjärvi	3578529	6944881	09.06.2017	No	QFB gneiss	moderate foliation				358	72	no aeroEM anomaly

2017-ME-097	Rääpysjärvi	3578472	6944656	09.06.2017	No	QFB gneiss	moderate foliation, slightly deformed				212	50	quartz clusters and veins along foliation, 160m S same rock, no aeroEM anomaly
2017-ME-098	Rääpysjärvi	3578616	6944372	09.06.2017	Yes	Garnet bearing QFB gneiss	moderate foliation, slightly deformed				320	68	slightly rusty, quartz veins along foliation, no aeroEM anomaly
2017-ME-099	Rääpysjärvi	3578471	6944290	09.06.2017	Yes	Garnet bearing QFB gneiss	moderate foliation	graphite	traces of graphite, disseminated, flake size 1-2mm	<1%			Contains few green large mineral grains in leukosome, moderate aeroEM anomaly
2017-ME-100	Rääpysjärvi	3578131	6944303	09.06.2017	No	QFB gneiss	weak to moderate foliation, homogenous	graphite	traces of graphite, disseminated, flake size 1-2mm	<1%	330	68	structural measurement might be off because of difficulty to measure on that particular outcorp, weak aeroEM anomaly
2017-ME-101	Rääpysjärvi	3578188	6944506	09.06.2017	No	QFB gneiss	moderate foliation, homogenous				228	66	no aeroEM anomaly
2017-ME-102	Rääpysjärvi	3577696	6944768	09.06.2017	No	QFB gneiss	moderate foliation, banded, very deformed						PICTURE HAS WRONG NUMBER (101) hammer is used for scale in this picture, no aeroEM anomaly
2017-ME-103	Rääpysjärvi	3577506	6944832	09.06.2017	Yes	Graphite schist	moderate foliation		disseminated, flake size 1mm	2 %			rusty and brittle, no aeroEM anomaly

2017-ME-104	Rääpysjärvi	3575301	6945434	10.09.2017	No	QFB gneiss	moderate foliation						nothing but round and subangular boulders in this area, most are QFB gneiss, strong aeroEM anomaly
2017-ME-105	Rääpysjärvi	3575044	6945260	10.09.2017	No	QFB gneiss	moderate foliation				230	72	weak aeroEM anomaly
2017-ME-106	Rääpysjärvi	3575259	6945200	10.09.2017	Yes	QFB gneiss	moderate foliation, very deformed, migmatitic						too deformed for structural measurements, strong aeroEM anomaly
2017-ME-107	Rääpysjärvi	3576063	6945061	10.09.2017	Yes	QFB gneiss	weak to moderate foliation, homogenous	graphite	disseminated, flakes up to 1mm	1-2%	310	70	rusty, stron aeroEM anomaly
2017-ME-108	Rääpysjärvi	3575756	6944660	10.09.2017	No	Garnet bearing QFB gneiss	moderate foliation						only boulders in the area, no aeroEM anomaly
2017-ME-109	Rääpysjärvi	3577678	6944990	10.09.2017	No	QFB gneiss	moderate foliation, deformed, migmatitic				282	70	no aeroEM anomaly
2017-ME-110	Rääpysjärvi	3576998	6946312	11.06.2017	Yes	Graphite schist	weak foliation, homogenous	graphite	disseminated and patchy, flake size up to 3mm	4 %			rusty, slightly sulfidic, many angular graphite schist boulders in the area, no aeroEM anomaly
2017-ME-111	Rääpysjärvi	3576901	6946406	11.06.2017	No	QFB gneiss	weak to moderate, deformed, migmatitic				208	32	coarse grained quartz clusters, structural measurement

													unreliable, no aeroEM anomaly
2017-ME-112	Rääpysjärvi	3577189	6946538	11.06.2017	No	QFB gneiss	moderate foliation				312	72	no aeroEM anomaly
2017-ME-113	Rääpysjärvi	3577447	6946256	11.06.2017	Yes	Garnet bearing QFB gneiss	moderate foliation				324	80	quartz veins along foliation, strong aeroEM anomaly
2017-ME-114	Rääpysjärvi	3577418	6946209	11.06.2017	Yes	Graphite schist	moderate foliation, homogenous	graphite	disseminated, flakes up to 4mm	4 %	326	80	rusty, sulfidic, brittle, very weathered, strong aeroEM anomaly
2017-ME-115	Rääpysjärvi	3577828	6946005	11.06.2017	No	QFB gneiss	weak foliation, migmatitic				220	80	partly QFB gneiss, granite contains mafic flames, coarse grained quartz clusters, no aeroEM anomaly
2017-ME-116	Rääpysjärvi	3578148	6945791	11.06.2017	Yes	Garnet bearing QFB gneiss	moderate foliation	graphite	disseminated, flake size 3-5mm	1 %			slightly rusty, moderate to strong aeroEM anomaly
2017-ME-117	Rääpysjärvi	3578577	6945656	11.06.2017	Yes	QFB gneiss	moderate foliation				300	50	no aeroEM anomaly
2017-ME-118	Rääpysjärvi	3578078	6945513	11.06.2017	Yes	QFB gneiss	moderate foliation	graphite	disseminated, enriched in mica rich parts, flake size 2-4mm	1 %			rusty, sulfidic, brittle, no aeroEM anomaly
2017-ME-119	Rääpysjärvi	3577726	6945815	11.06.2017	No	Garnet bearing QFB gneiss	moderate foliation, deformed, banded				246	64	thick quartz veins along foliation, no aeroEM anomaly
2017-ME-120	Rääpysjärvi	3577640	6946227	11.06.2017	No	QFB gneiss	weak foliation, deformed	graphite	traces of graphite, disseminated	<1%			slightly rusty, no aeroEM anomaly

2017-ME-121	Rääpysjärvi	3576796	6944429	12.06.2017	No	Garnet bearing QFB gneiss	moderate foliation, slightly deformed				336	88	no aeroEM anomaly
2017-ME-122	Rääpysjärvi	3576798	6943994	12.06.2017	No	QFB gneiss	moderate foliation, slighlty deformed				330	78	no aeroEM anomaly
2017-ME-123	Rääpysjärvi	3576623	6943881	12.06.2017	Yes	QFB gneiss	moderate foliation				204	78	no aeroEM anomaly
2017-ME-124	Rääpysjärvi	3576752	6944373	12.06.2017	No	Garnet bearing QFB gneiss	moderate foliation, slightly deformed				298	72	same rock 100m ESE, no aeroEM anomaly
2017-ME-125	Rääpysjärvi	3578412	6945101	12.06.2017	No	QFB gneiss	very deformed, migmatitic						too deformed for structural measurements, no aeroEM anomaly
2017-ME-126	Rääpysjärvi	3578420	6945057	12.06.2017	Yes	Graphite schist	moderate foliation	graphite	disseminated, 1-2mm flakes	2 %	250	62	rusty, sulfidic, weathered, pretty hard, contains white fibruous minerals, possibly asbestos?, mapped as serpentinite according to GTK, no aeroEM anomaly
2017-ME-127	Kohmansalo	3576369	6941960	27.06.2017	No	QFB gneiss	weak foliation, deformed						too deformed for structural measurements, granite veins with ptygmatic folds, no aeroEM anomaly

2017-ME-128	Kohmansalo	3576260	6941961	27.06.2017	No	QFB gneiss	moderate foliation, banded				216	68	coarse grained quartz veins along foliation, weak aeroEM
2017-ME-129	Kohmansalo	3576097	6941893	27.06.2017	Yes	QFB gneiss	weak foliation						granite veins with ptygmatic folds and small boudinage, coarse grained quartz clusters, strong aeroEM anomaly
2017-ME-130	Kohmansalo	3576085	6941737	27.06.2017	Yes	Garnet bearing QFB gneiss	moderate foliation	graphite	disseminated, 1-2mm flakes	<1%	216	52	strong aeroEM anomaly
2017-ME-131	Kohmansalo	3576144	6941613	27.06.2017	Yes	QFB gneiss	weak foliation, very deformed, very migmatitic	graphite	disseminated, enriched in mica rich parts, 1-2mm flakes	1-2%	216	58	slightly rusty mica rich parts, moderate aeroEM anomaly
2017-ME-132	Kohmansalo	3576082	6941510	27.06.2017	No	QFB gneiss	moderate foliation, very deformed, migmatitic						too deformed for structural measurements, no aeroEM anomaly
2017-ME-133	Kohmansalo	3576270	6941302	27.06.2017	Yes	QFB gneiss	moderate foliation, deformed, migmatitic	graphite	traces of graphite, disseminated, 1-2mm flakes	<1%	218	68	no aeroEM anomaly
2017-ME-134	Kohmansalo	3576645	6941593	27.06.2017	No	QFB gneiss	moderate foliation				220	70	quartz veins along foliation, no aeroEM anomaly
2017-ME-135	Kohmansalo	3576556	6941568	27.06.2017	Yes	Graphite schist	weak foliation	graphite	disseminated, 1mm flakes	2-3%			multiple boulders to the W along road,

													weak aeroEM anomaly
2017-ME-136	Kohmansalo	3576448	6941843	27.06.2017	No	QFB gneiss	moderate foliation, slightly deformed				200	70	PICTURE HAS WRONG NUMBER (135), no aeroEM anomaly
2017-ME-137	Kohmansalo	3577593	6940734	28.06.2017	No	QFB gneiss	weak foliation, very migmatitic	graphite	traces of graphite, disseminated, 1mm flakes	<1%	206	72	140m W same rock, no aeroEM anomaly
2017-ME-138	Kohmansalo	3577310	6940845	28.06.2017	No	QFB gneiss	moderate foliation, migmatitic, banded				194	68	slightly rusty, no aeroEM anomaly
2017-ME-139	Kohmansalo	3577370	6941001	28.06.2017	Yes	Graphite schist	weak foliation	graphite	disseminated, patchy, 1-2mm flakes	2 %			rusty, sulfidic, brittle, strong aeroEM anomaly
2017-ME-140	Kohmansalo	3577159	6940961	28.06.2017	No	QFB gneiss	moderate foliation, slightly deformed						at places migmatitic, foliation follows general trend around 200/70, 120m NW same rock
2017-ME-141	Kohmansalo	3576977	6941309	28.06.2017	No	QFB gneiss	weak foliation, homogenous						foliation too weak to measure, granite veins with ptygmatic folds, strong aeroEM anomaly
2017-ME-142	Kohmansalo	3577057	6941412	28.06.2017	Yes	QFB gneiss	moderate foliation, banded				204	80	quartz veins along foliation, moderate aeroEM anomaly

2017-ME-143	Kohmansalo	3577753	6941164	28.06.2017	No	QFB gneiss	moderate foliation, slightly deformed				186	74	100m NW same rock, weak aeroEM anomaly
2017-ME-144	Kohmansalo	3577875	6940575	28.06.2017	Yes	QFB gneiss	moderate foliation	graphite	disseminated, 1mm flakes	1 %	218	72	quartz veins along foliation, strong aeroEM anomaly
2017-ME-145	Kohmansalo	3577946	6940461	28.06.2017	No	Garnet bearing QFB gneiss	moderate foliation, slightly deformed				210	66	quartz veins and clusters along foliation, strong aeroEM anomaly
2017-ME-146	Kohmansalo	3577665	6940762	29.06.2017	Yes	QFB gneiss	weak foliation, slightly deformed, migmatitic	graphite	disseminated, patchy, 2-3mm flakes	1 %	200	66	slightly rusty, quartz clusters, modreate aeroEM anomaly
2017-ME-147	Kohmansalo	3577735	6940512	29.06.2017	No	QFB gneiss	moderate foliation				180	64	quartz veins along foliation, moderate to strong aeroEM anomaly
2017-ME-148	Kohmansalo	3577843	6940292	29.06.2017	Yes	Graphite schist	moderate foliation	graphite	disseminated, <1mm flakes	3-4%			rusty, brittle, slightly sulfidic, strong aeroEM anomaly
2017-ME-149	Kohmansalo	3577848	6940308	29.06.2017	Yes	Graphite schist	moderate foliation	graphite	patchy and enriched in layers, disseminated in side rock, 1-2mm flakes	5 %	258	60	rusty, slightly sulfidic, brittle, soft, 30cm wide graphite schist horizon, the siderock conatins disseminated graphite, 50m NW of site another outcrop with a graphite schist horizon, possibly a

													continuation of the same, strong aeroEM anomaly
2017-ME-150	Kohmansalo	3577895	6940127	29.06.2017	No	QFB gneiss	moderate foliation				230	70	moderate aeroEM anomaly
2017-ME-151	Kohmansalo	3578054	6939979	29.06.2017	No	QFB gneiss	moderate foliation, slightly deformed				200	70	moderate aeroEM anomaly
2017-ME-152	Kohmansalo	3578253	6940166	29.06.2017	No	QFB gneiss	moderate foliation, migmatitic				208	78	at places migmatitic, weak aeroEM anomaly
2017-ME-153	Kohmansalo	3578126	6940219	29.06.2017	Yes	QFB gneiss	moderate foliation, slightly deformed	graphite	disseminated, 1-2mm flakes	1 %	194	62	strong aeroEM anomaly
2017-ME-154	Kohmansalo	3578175	6940375	29.06.2017	No	QFB gneiss	moderate foliation				194	68	quartz veins along foliation, weak aeroEM anoamly
2017-ME-155	Kohmansalo	3579315	6940756	30.06.2017	No	QFB gneiss	moderate foliation	graphite	traces of graphite, disseminated, 1-2mm flakes	<1%	192	82	slightly rusty, quartz veins along foliation, strong aeroEM anomaly
2017-ME-156	Kohmansalo	3579386	6941063	30.06.2017	No	QFB gneiss	very migmatitic, very deformed						PICTURE HAS WRONG NUMBER (155), too deformed for structural measurements, weak aeroEM anomaly
2017-ME-157	Kohmansalo	3579069	6940999	30.06.2017	No	QFB gneiss	weak foliation, very deformed						slightly rusty, too deformed for structural measurements,

													quartz clusters, 100m S same rock, moderate aeroEM anomaly
2017-ME-158	Kohmansalo	3579054	6940969	30.06.2017	Yes	Graphite schist	moderate foliation	graphite	disseminated, 1mm flakes	2 %			PICTURE HAS WRONG NUMBER (157) (compass used for scale here) rusty, sulfidic, contains apatite and white fibruous minerals, possibly asbestos?, feels like magnesium powder on fingers, moderate aeroEM anomaly
2017-ME-159	Kohmansalo	3578991	6940710	30.06.2017	Yes	Garnet bearing QFB gneiss	moderate foliation				200	62	quartz clusters, at places deformed, no aeroEM anomaly
2017-ME-160	Kohmansalo	3579134	6940667	30.06.2017	No	QFB gneiss	moderate foliation, slightly deformed				190	64	quartz veins along foliation, 100m SE same rock, moderate to strong aeroEM anomaly
2017-ME-161	Kohmansalo	3579240	6940398	30.06.2017	No	QFB gneiss	moderate foliation, slightly deformed				210	70	quartz veins along foliation, weak aeroEM anomaly
2017-ME-162	Kohmansalo	3579498	6940436	30.06.2017	No	QFB gneiss	moderate foliation				210	68	quartz veins along foliation, 300m E same rock, strong aeroEM anomaly

2017-ME-163	Kohmansalo	3579893	6940516	30.06.2017	Yes	Graphite schist	weak foliation	graphite	disseminated, patchy, 1mm flakes	4 %			rusty, sulfidic, brittle, visible pyrite crystalls at some boulders, weak aeroEM anomaly
2017-ME-164	Kohmansalo	3579929	6940524	30.06.2017	No	QFB gneiss	moderate foliation				216	68	quartz veins along foliation, weak aeroEM anomaly
2017-ME-165	Kohmansalo	3579686	6940722	30.06.2017	No	QFB gneiss	moderate foliation, slightly deformed				190	72	quartz clusters and veins along foliation, 250m W same rock, moderate aeroEM anomaly
2017-ME-166	Kohmansalo	3576221	6941721	02.07.2017	Yes	Graphite schist	moderate to strong foliation	graphite	disseminated, patchy, 1-2mm flakes	5 %	240	62	very rusty, slightly sulfidic, foliation difficult to measure due to rustyness, whole outcrop is graphite schist with a size of 30x50m, strong aero and minislingramEM anomaly
2017-ME-167	Kohmansalo	3576177	6941699	02.07.2017	No	QFB gneiss	moderate foliation				220	68	50m S of previous graphite schist site, strong minislingramEM anomaly
2017-ME-168	Kohmansalo	3577583	6940878	02.07.2017	Yes	QFB gneiss	moderate foliation	graphite	disseminated, patchy, enriched in mica rich parts, 2-3mm flakes	2-3%	242	58	rusty, soft at places, slightly sulfidic and brittle, weathered, moderate to strong

													minislingramEM anomaly
2017-ME-169	Kohmansalo	3577448	6940885	02.07.2017	No	QFB gneiss	moderate foliation	graphite	disseminated, 1-2mm flakes	<1%	220	64	slightly rusty, moderate minislingramEM anomaly
2017-ME-170	Kohmansalo	3577660	6940690	02.07.2017	Yes	Graphite schist	moderate to strong foliation	graphite	disseminated, 1-2mm flakes	5-8%	250	58	boulder very local, contains white fibruous minerals, possibly asbestos?, site dead on GTKs interpreted black shale line, strong minislingramEM anomaly
2017-ME-171	Kohmansalo	3577841	6940316	02.07.2017	Yes	Graphite schist	moderate foliation	graphite	disseminated, 1-2mm flakes	5 %	230	62	rusty, sulfidic, soft, whole point of ridge is graphite schist, 40x10m, contains white fibruous mienrals, possibly asbestos?, strong minislingramEM anomaly
2017-ME-172	Kohmansalo	3577802	6940356	02.07.2017	Yes	QFB gneiss	moderate foliation, slightly deformed, mylonitic				230	70	rusty mica rich parts, strong shearing?, rounded plagioclase and quartz clasts in fine grained mafic matrix, moderate to weak minislingramEM anomaly

2017-ME-173	Kohmansalo	3577998	6940373	02.07.2017	No	QFB gneiss	moderate foliation, slightly mylonitic				220	68	slightly rusty, weak minislingramEM anomaly
2017-ME-174	Kohmansalo	3579329	6940801	04.07.2013	No	QFB gneiss	moderate foliation, slightly deformed				190	70	slightly rusty at places, quartz clusters, moderate minislingramEM anomaly
2017-ME-175	Kohmansalo	3579349	6940671	04.07.2013	Yes	QFB gneiss	weak foliation, homogenous	graphite	disseminated, 1mm flakes	<1%			rusty, heavy, contains pyrite and other sulfides, weak minislingramEM anomaly
2017-ME-176	Kohmansalo	3579317	6940586	04.07.2013	Yes	Graphite schist	moderate foliation	graphite	disseminated, <1mm flakes	4 %	250	70	very rusty, structural measurements difficult to measure, strong minislingramEM anomaly
2017-ME-177	Kohmansalo	3579233	6940784	04.07.2013	Yes	QFB gneiss	moderate foliation	graphite	traces of graphite, disseminated, 1-2mm flakes	<1%	210	80	very rusty, sulfidic, quartz clusters, contains apatite, weak minislingramEM anomaly
2017-ME-178	Kohmansalo	3579452	6940530	04.07.2013	No	QFB gneiss	moderate foliation	graphite	traces of graphite, enriched in mica rich parts, 1mm flakes	<1%	186	76	slightly rusty, weak to no minislingramEM anomaly
2017-ME-179	Kohmansalo	3579625	6940449	04.07.2013	Yes	Graphite schist	moderate foliation	graphite	disseminated, patchy, 1-2mm flakes	5-8%			rusty, sulfidic, brittle, heavy,

													contains pyrite, chalcopyrite? And possibly more sulfides, sulfide content ~10%, moderate minislingramEM anomaly
2017-ME-180	Kohmansalo	3579671	6940371	04.07.2013	Yes	QFB gneiss	weak foliation	graphite	patchy, 1-2mm flakes	1 %	260	68	very rusty, weathered, structural measurements difficult to measure, strong minislingramEM anomaly

Appendix B

Micro-XRF data used for pseudosections. Analysis conducted by lab engineer Sören Fröjdö at Geology and mineralogy, Åbo Akademi University.

XRF-data											
Sample #	SiO2(%)	TiO2(%)	Al2O3(%)	Fe2O3(%)	MnO(%)	MgO(%)	CaO(%)	K2O(%)	Na2O(%)	P2O5(%)	SUM
083	71,248	0,613	12,875	5,614	0,064	2,096	1,962	2,187	2,397	0,154	99,21
015	70,101	0,579	13,194	6,118	0,192	2,087	6,523	0,417	0,336	0,166	99,713

Appendix C

Microprobe data from garnet-biotite pairs.

29_bt

From w%	1	2	3	4	5	Average
SiO2	32.94	32.24	32.84	33.52	30.72	32.45
TiO2	2.94	2.94	2.94	2.94	2.94	2.94
Al2O3	20.01	20.01	20.01	20.01	20.01	20.01
Fe2O3	19.23	18.87	18.47	17.96	18.23	18.55
MgO	10.79	10.58	10.77	10.77	10.44	10.67
Na2O	0.49	0.49	0.49	0.49	0.49	0.49
K2O	10.19	10.19	10.19	10.19	10.19	10.19
SUM	96.58	95.32	95.70	95.88	93.01	

29_grt

From w%	1	2	3	4	5	Average
SiO2	40.48	41.39	40.73	39.95	41.27	40.76
Al2O3	22.75	22.75	22.75	22.75	22.75	22.75
Fe2O3	34.37	33.93	34.07	33.43	33.96	33.95
MnO	7.30	7.30	7.30	7.30	7.30	7.30
MgO	3.23	3.17	3.28	3.24	3.08	3.20
CaO	1.13	1.13	1.13	1.13	1.13	1.13
SUM	109.25	109.67	109.27	107.79	109.48	

83_bt

From w%	1	2	3	4	5	Average
SiO2	32.94	33.71	33.70	33.96	34.11	33.68
TiO2	2.29	2.29	2.29	2.29	2.29	2.29
Al2O3	19.93	19.93	19.93	19.93	19.93	19.93
Fe2O3	18.38	18.37	17.10	18.51	18.07	18.09
MgO	10.94	11.44	10.71	11.26	11.15	11.10
Na2O	0.38	0.38	0.38	0.38	0.38	0.38
K2O	10.23	10.23	10.23	10.23	10.23	10.23
SUM	95.09	96.35	94.33	96.54	96.16	

83_grt

From w%	1	2	3	4	5	Average
SiO2	41.04	40.77	41.80	40.18	40.72	40.90
Al2O3	22.52	22.52	22.52	22.52	22.52	22.52
Fe2O3	37.05	36.75	37.08	36.70	35.58	36.63
MnO	3.71	3.71	3.71	3.71	3.71	3.71
MgO	3.42	3.45	3.42	3.16	3.56	3.40
CaO	1.09	1.09	1.09	1.09	1.09	1.09
SUM	108.83	108.29	109.62	107.37	107.19	

113_bt

From w%	1	2	3	4	5	Average
SiO2	34.00	33.69	33.30	34.10	32.99	33.62
TiO2	2.32	2.32	2.32	2.32	2.32	2.32
Al2O3	19.75	19.75	19.75	19.75	19.75	19.75
Fe2O3	19.04	18.90	19.10	19.34	19.18	19.11
MgO	10.66	10.69	10.81	11.00	10.73	10.78
Na2O	0.39	0.39	0.39	0.39	0.39	0.39
K2O	9.77	9.77	9.77	9.77	9.77	9.77
SUM	95.93	95.51	95.43	96.67	95.13	

113_grt

From w%	1	2	3	4	5	Average
SiO2	41.76	40.56	38.75	42.41	41.25	40.95
Al2O3	23.22	23.22	23.22	23.22	23.22	23.22
Fe2O3	35.73	35.39	35.81	35.69	35.08	35.54
MnO	4.74	4.74	4.74	4.74	4.74	4.74
MgO	3.32	3.09	2.99	2.94	2.79	3.03
CaO	1.25	1.25	1.25	1.25	1.25	1.25
SUM	110.01	108.26	106.75	110.25	108.32	

177_bt

From w%	1	2	3	4	5	Average
SiO2	32.85	22.88	33.38	33.78	33.77	31.33
TiO2	1.80	1.80	1.80	1.80	1.80	1.80
Al2O3	21.28	21.28	21.28	21.28	21.28	21.28
Fe2O3	18.21	18.17	17.20	17.61	17.18	17.67
MgO	9.93	9.51	10.62	10.35	10.49	10.18
Na2O	0.50	0.50	0.50	0.50	0.50	0.50
K2O	11.13	11.13	11.13	11.13	11.13	11.13
SUM	95.69	85.27	95.90	96.45	96.15	

177_grt

From w%	1	2	3	4	5	Average
SiO2	39.83	42.13	41.17	40.54	41.78	41.09
Al2O3	24.00	24.00	24.00	24.00	24.00	24.00
Fe2O3	28.75	29.64	28.85	28.70	28.48	28.88
MnO	8.74	8.74	8.74	8.74	8.74	8.74
MgO	2.64	3.07	2.59	2.58	2.47	2.67
CaO	1.29	1.29	1.29	1.29	1.29	1.29
SUM	105.25	108.87	106.64	105.84	106.76	

Appendix D

Microprobe data recalculated to cations as used in thermometric calculation sheet.

	29_Garnet					29_Biotite			
	Fe	Mn	Mg	Ca		Ti	Al-vi	Fe	Mg
avg	1.780	0.431	0.332	0.085		0.164	1.433	1.034	1.178
1	1.803	0.431	0.335	0.085		0.162	1.430	1.058	1.177
2	1.767	0.428	0.327	0.084		0.164	1.445	1.053	1.170
3	1.784	0.430	0.341	0.085		0.163	1.419	1.024	1.183
4	1.775	0.436	0.341	0.086		0.162	1.382	0.990	1.177
5	1.772	0.428	0.318	0.084		0.168	1.491	1.045	1.186

	83_Garnet					83_Biotite			
	Fe	Mn	Mg	Ca		Ti	Al-vi	Fe	Mg
avg	1.919	0.219	0.353	0.081		0.126	1.402	0.999	1.214
1	1.933	0.218	0.354	0.081		0.127	1.433	1.024	1.208
2	1.926	0.219	0.358	0.081		0.125	1.415	1.009	1.244
3	1.917	0.216	0.350	0.080		0.128	1.372	0.955	1.185
4	1.942	0.221	0.331	0.082		0.125	1.404	1.014	1.221
5	1.879	0.220	0.372	0.082		0.125	1.387	0.992	1.212

	133_Garnet					113_Biotite			
	Fe	Mn	Mg	Ca		Ti	Al-vi	Fe	Mg
avg	1.856	0.279	0.313	0.093		0.128	1.405	1.055	1.179
1	1.841	0.275	0.339	0.091		0.128	1.385	1.048	1.162
2	1.857	0.280	0.322	0.093		0.128	1.395	1.045	1.171
3	1.916	0.285	0.316	0.095		0.129	1.418	1.059	1.188
4	1.832	0.274	0.299	0.091		0.127	1.396	1.057	1.191
5	1.835	0.279	0.289	0.093		0.129	1.429	1.068	1.184

	177_Garnet					177_Biotite			
	Fe	Mn	Mg	Ca		Ti	Al-vi	Fe	Mg
avg	1.535	0.523	0.281	0.097		0.102	1.532	1.004	1.146
1	1.552	0.531	0.283	0.099		0.100	1.147	1.012	1.093
2	1.542	0.512	0.317	0.095		0.116	1.923	1.172	1.215
3	1.533	0.523	0.272	0.097		0.099	1.451	0.950	1.162
4	1.538	0.527	0.273	0.098		0.099	1.437	0.967	1.126
5	1.507	0.521	0.259	0.097		0.099	1.432	0.945	1.143